geosciences

MDPI

Article

Provenance of the Papuan Peninsula (Papua New Guinea): Zircon Inheritance from Miocene–Pliocene Volcanics and Volcaniclastics

Robert J. Holm [1,*], Kelly Heilbronn [1], Dulcie Saroa [2] and Gideon Maim [2]

[1] Geosciences, College of Science & Engineering, James Cook University, Townsville, QLD 4811, Australia
[2] Geological Survey Division, Mineral Resources Authority, Port Moresby 121, Papua New Guinea
* Correspondence: robert.holm@goldfields.com

Abstract: Plate tectonic reconstructions of Papua New Guinea prior to the late Cenozoic are characterized by a lack of provenance data to constrain the relative origin of the allochthonous terranes. At present, plate tectonic reconstructions of this region infer that the accreted New Guinea terranes at the northern Australian continental margin are likely autochthonous or para-autochthonous in nature. This study presents the results of an investigation into zircons derived from Miocene–Pliocene volcanics and volcaniclastics of the Papuan Peninsula. Results from U-Pb zircon geochronology inform the recent geological history of the Papuan Peninsula, with magmatism active in the late Miocene and early Pliocene, between approximately 9 Ma and 4.5 Ma. More significantly, however, is the recognition of extensive inherited zircon grains within the volcanic and volcaniclastic sequences. These inherited zircon grains are most likely sourced from the Owen Stanley Metamorphics, which form the basement rocks of the Papuan Peninsula. Provenance of the inherited zircon grains imply that the Cretaceous volcaniclastic protolith of the Owen Stanley Metamorphics must have had input from continental detritus, but this cannot be derived from North Queensland, Australia as inferred by current reconstructions. Instead, zircon U-Pb age spectra correlate with probable source regions further to the south, adjacent to the Shoalwater Formation of the Central Queensland margin, and New Caledonia. These findings suggest that late Mesozoic and Cenozoic regional reconstructions of eastern Australia and the Southwest Pacific require major revision and that additional work is undertaken to inform the provenance of such allochthonous terranes.

Keywords: Papua New Guinea; Southwest Pacific; volcanic; volcaniclastic; zircon; U-Pb dating; provenance

check for updates

Citation: Holm, R.J.; Heilbronn, K.; Saroa, D.; Maim, G. Provenance of the Papuan Peninsula (Papua New Guinea): Zircon Inheritance from Miocene–Pliocene Volcanics and Volcaniclastics. *Geosciences* **2023**, *13*, 324. https://doi.org/10.3390/geosciences13110324

Academic Editors: Jesus Martinez-Frias and Angelos G. Maravelis

Received: 30 June 2023
Revised: 15 October 2023
Accepted: 16 October 2023
Published: 25 October 2023

Copyright: © 2023 by the authors. Licensee MDPI, Basel, Switzerland. This article is an open access article distributed under the terms and conditions of the Creative Commons Attribution (CC BY) license (https://creativecommons.org/licenses/by/4.0/).

1. Introduction

Papua New Guinea is located in a complex tectonic intersection between the Australian continent, the Southwest Pacific, and Southeast Asia. Resolving the plate tectonic evolution of this region has proven difficult to date due to the plethora of contradicting geologic models that stem from a lack of constraining regional datasets. However, a growing body of analytical data over recent decades has led to a progressive shift in our understanding of the plate tectonic history. For example, tectonic models of New Guinea have progressed from a largely autochthonous or para-autochthonous terrane model [1–3] to one of allochthonous terranes that accreted to the northern margin of the Australian continent [4–6].

Although it is now generally accepted that New Guinea formed via accretion tectonics at the northern margin of the Australian continent, there is insufficient work to establish the origin of these terranes. Provenance studies to date have been limited in both scope and spatial distribution [7–9]. Such limitations have led authors of previous reconstructions for Papua New Guinea to interpret the location of the Papuan Peninsula close to that of the present day—adjacent to northeast Australia (Figure 1)—throughout the Cretaceous and early Cenozoic [3,5,10–12]. These reconstructions infer that the Papuan Peninsula formed

together with the Eastern and Papuan plateaus of the northwest Coral Sea, and that these terranes were transported northward relative to Australia by opening of the Coral Sea in the Paleocene and early Eocene [13]. Such an autochthonous or para-autochthonous terrane model has formed the accepted plate tectonic interpretation for the region. This is despite the presence of a younger fossil subduction zone between the Papuan Peninsula and Coral Sea [14–16]; no conclusive studies to test the link between the basement of the Papuan Peninsula and the northwest Coral Sea plateaus, nor the provenance of the Papuan Peninsula against northeast Australia have been performed.

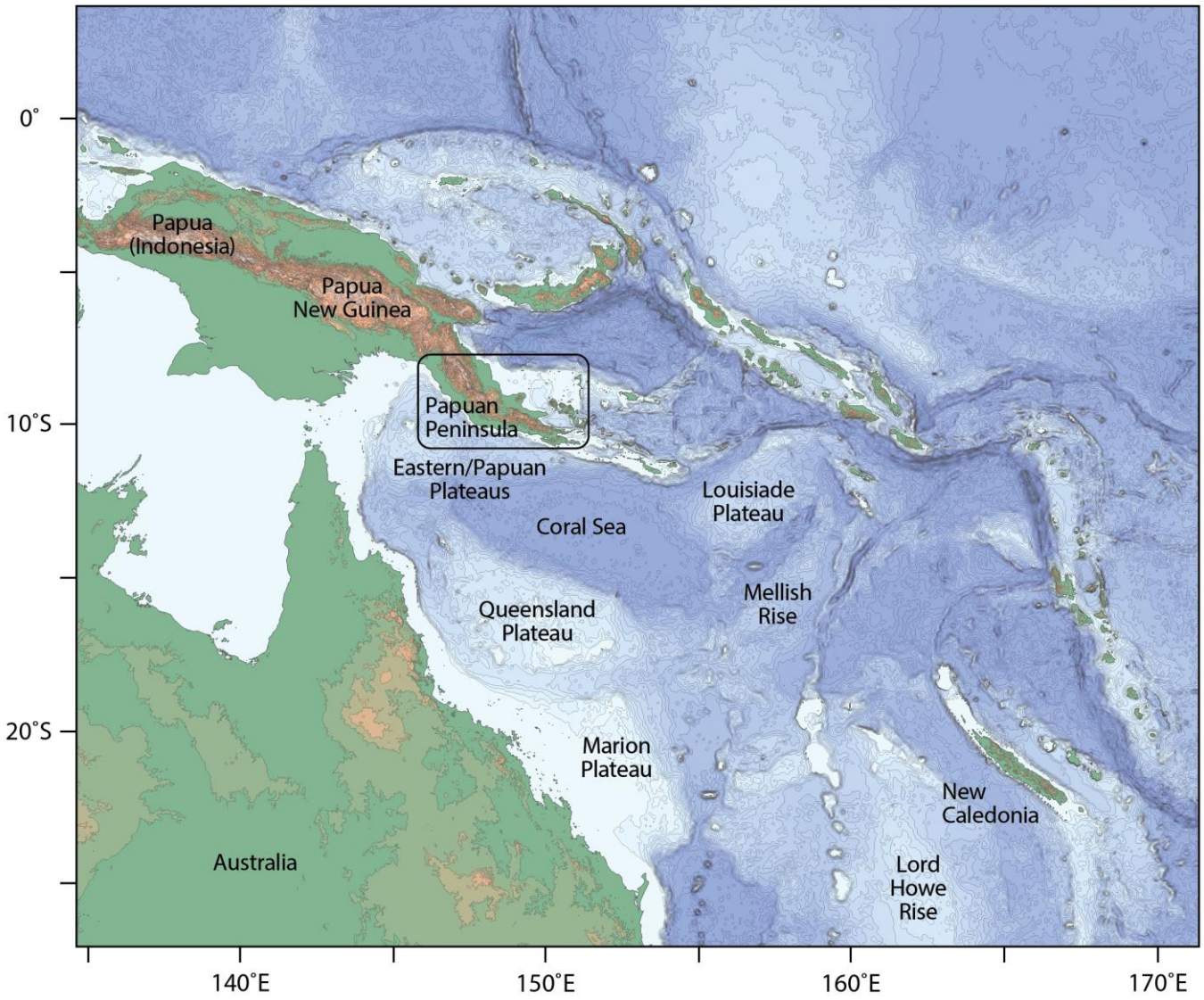

Figure 1. Location of the study area in the wider Southwest Pacific. Rectangle indicates area of focus and sampling in the Papuan Peninsula of Papua New Guinea; see Figure 2 and Table 1 for more details.

Table 1. Location details and description of samples used for this study. All coordinates are in WGS84-UTM Zone 55.

Sample	Formation	Easting	Northing	Locality	Brief Description
103021	Mt Davidson Volcanics	480508	9046783	Bakoiudu Village roadside	Coarse-grained volcaniclastic sandstone; deeply weathered with relict plagioclase, amphibole and biotite.
103220	Mt Davidson Volcanics	484681	9056640	Tapini Highway, Jailobo–Ninifi 2	Medium-grained volcaniclastic sandstone with intermediate volcanic pebble clasts, plagioclase, biotite and minor quartz.
103252	Yaifa Formation	484973	9060133	Ninifi 1, Mona Highway	Highly degraded mudstone to claystone; no thin section.
103253	Yaifa Formation	484952	9059892	Ninifi 2, Mona Highway	Highly degraded sandstone to mudstone; no thin section.
103254A	Apinaipi Formation	466423	9035278	Mona Highway	Matrix-supported pebble to cobble conglomerate with clasts comprising intermediate volcanics.
103256	Apinaipi Formation	466423	9035278	Mona Highway	Tuffaceous sandstone with intermediate volcanic pebble clasts, and plagioclase and biotite fragments.
103257	Yaifa Formation	496928	9006075	Doa Plantation	Mudstone to siltstone with minor shards of biotite.
103258	Yaifa Formation	496928	9006075	Doa Plantation	Fine-grained tuffaceous sandstone; plagioclase, biotite and pyroxene; minor volcanic pebble clasts.
103259	Mt Davidson Volcanics	498999	9005213	Doa Plantation	Basaltic volcanic agglomerate; clasts predominantly comprise porphyritic basalt with phenocrysts of plagioclase, and pyroxene.
103261	Astrolabe Agglomerate	542733	8958003	Rouna Power Station 2	Basaltic volcanic agglomerate; clasts predominantly comprise porphyritic basalt with phenocrysts of plagioclase and olivine.
103271	Kore Volcanics	591677	8893242	Kore Village roadside	Clast of porphyritic basaltic andesite derived from volcanic conglomerate.
103272	Kore Volcanics	591677	8893242	Kore Village roadside	Clast of basalt derived from volcanic conglomerate.
103273	Kore Volcanics	591736	8893276	Kore Village roadside	Tuffaceous sandstone with basaltic pebble clasts, and plagioclase, olivine and pyroxene fragments.

In this study we report the results of an investigation into Miocene–Pliocene volcanic and volcaniclastic rocks of the Papuan Peninsula. New U-Pb zircon geochronology results are used to determine the maximum depositional age for the volcanic and volcaniclastic successions, however, the same rocks also yielded unexpected populations of inherited zircon grains. Analysis of inherited zircon grains can provide a powerful means of resolving the provenance history of potentially displaced terranes [17]; we therefore compare the resulting age distribution of the Papuan Peninsula units with the zircon age spectra and crustal history of possible source regions. The results from this work provide valuable data constraining the age for recent geologic events on the Papuan Peninsula, but also offer new insights into the provenance of the basement rocks of the Papuan Peninsula and challenge the currently accepted plate tectonic models for the region.

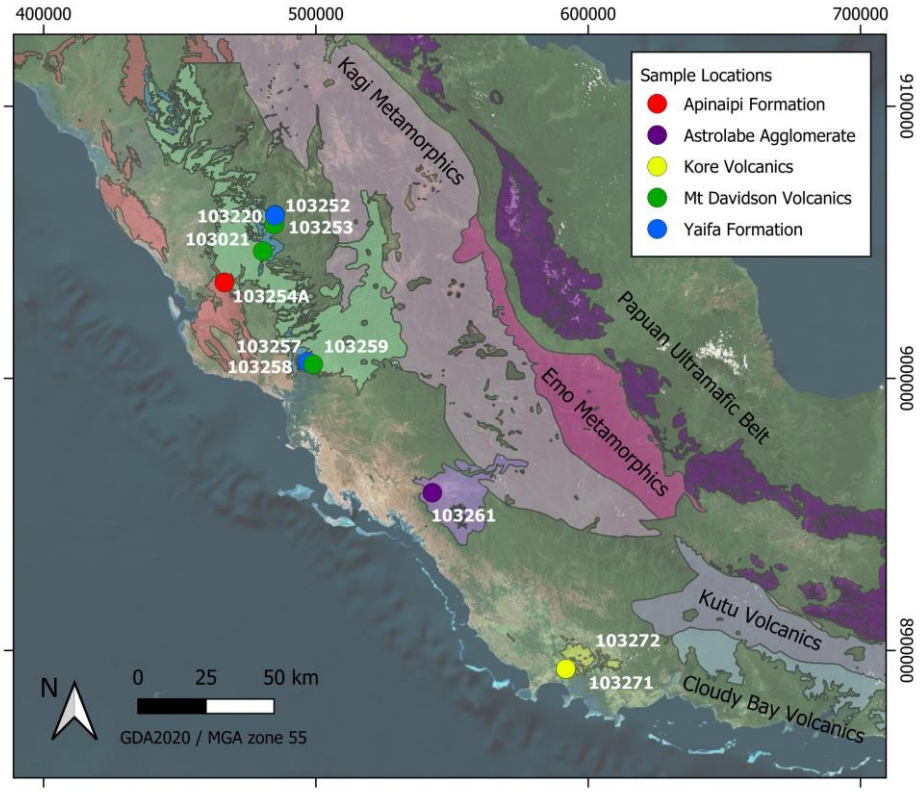

Figure 2. Geological map of the Papuan Peninsula study area and sample locations. The map shows key geological units of the Papuan Peninsula and the sampled units. Sample locations and descriptions are included in Table 1.

2. Geological Setting

The Papuan Peninsula, situated on the eastern part of the Papua New Guinea mainland between approximately 146° E and 151° E (Figures 1 and 2), consists of two main geological components: the Owen Stanley Metamorphic Complex in the south, transitioning to the Milne Terrane in the southeast, and the Papuan Ultramafic Belt, which makes up the northern half of the peninsula. The Owen Stanley Metamorphic Complex is comprised of two main rock units: the Kagi Metamorphics and the Emo Metamorphics. The Kagi Metamorphics are primarily composed of pelitic and psammitic volcaniclastics with minor intercalated volcanics. These rocks have undergone folding and metamorphism to greenschist facies [5,18]. The Emo Metamorphics overlie the Kagi Metamorphics in the northeast and form a 1–2 km thick carapace dipping shallowly to the north and northeast. The Emo Metamorphics consist mainly of metabasite derived from low-K tholeiitic basalt, dolerite, and gabbro, with minor volcaniclastic sediments [19,20]. This package of rocks was metamorphosed to greenschist and blueschist metamorphic facies [5,18]. The Owen Stanley Metamorphic Complex is interpreted to be of middle Cretaceous age based on U-Pb dating of zircon and preserved macrofossils [8,21,22].

Moving southeast, the Milne Terrane lies in an equivalent structural domain to the Owen Stanley Metamorphics and comprises the Goropu Metabasalt and Kutu Volcanics [19,20]. The Goropu Metabasalt consists of low-grade MORB-type metabasalts with minor intercalated metamorphosed limestone and calcareous schist. Submarine basaltic volcanics with interbedded lenses of pelagic limestone and minor terrigenous sediments form the interpreted protolith for the Goropu Metabasalt [20,23,24]. The Kutu Volcanics are considered the unmetamorphosed continuation of the Goropu Metabasalt and consist of predominantly basaltic lava with minor gabbro and ultramafics, along with agglomerate, tuffaceous, and calcareous sediments [20,23]. The depositional age of the Milne Terrane is constrained to the period between the Late Cretaceous (Maestrictian) and the Eocene [23].

The Papuan Ultramafic Belt is situated on the northeast side of the Papuan Peninsula, juxtaposed above the Owen Stanley Metamorphic Complex along the Owen Stanley Fault [5,25]. This belt is interpreted as an ophiolite complex consisting of oceanic crust and lithospheric mantle from the Late Cretaceous [5,26,27]. The obduction of the Papuan Ultramafic Belt and metamorphism of the Owen Stanley Metamorphic Complex occurred at 58.3 ± 0.4 Ma, derived from the cooling age of amphibole within the high-grade metamorphic contact between the two terranes [5,28].

The Papuan Peninsula was subsequently intruded by a major phase of subduction-related magmatism, which commenced during the middle Miocene and has continued to the present day [9,29–33]. The volcanic arc extends from the Papuan Peninsula southeastward through the D'Entrecasteaux Islands into the Louisiade Archipelago. It comprises various high-K calc-alkaline rocks, volcanic and plutonic shoshonite suites [30–32], predominantly basaltic andesite and andesite, and also includes basalt, dacite, and rhyolite with typical arc-type geochemical signatures [32]. This volcanic province shows a transition from early submarine-subaerial activity to entirely subaerial volcanism during the Pliocene and Quaternary periods, indicating the emergence of eastern Papua New Guinea during the latter part of the Cenozoic [5]. Additionally, the opening of the Woodlark Basin was accompanied by the introduction of peralkaline rhyolites along the northern side of the southeast Papuan Peninsula [33–35].

For more information on the Miocene–Pliocene units sampled in this study, please refer to the next section.

3. Samples

This study sampled five Miocene–Pliocene stratigraphic units of the Papuan Peninsula (Table 1; Figures 2–4; see also Figure A1 in Appendix A for sample photographs). The samples that comprise this study are derived from an array of volcanic–sedimentary environments. These form a representative population of different depositional settings, which are characterized by a wide spectrum of grain sizes and angularity. This sampling procedure accounts for variations in the size, shape, and concentration of detrital minerals, which may otherwise lead to bias in detrital zircon U-Pb age populations [36] through clustering or sorting influenced by the dynamics of sediment transport [37–40].

The Kore Volcanics are up to 250 m in thickness and comprise basaltic and andesitic pyroclastics, lava, volcanic sandstone with volcanic conglomerate towards the base, and lenses of marine tuff. The Kore Volcanics are interpreted to have been deposited during the Miocene as subaerial and shallow marine volcanics and pyroclastics [41]. Three samples from the Kore Volcanics are included in this study (Table 1; Figures 2–4): 103271 and 103272 are basaltic–andesite and basalt boulder clasts, respectively, derived from a volcanic conglomerate; sample 103273 is a tuffaceous sandstone with basaltic pebble clasts.

The upper Miocene to lower Pliocene Yaifa Formation comprises massive, tuffaceous sandstone with pebble horizons that grade through paraconglomerate into massive cobble conglomerate with tuffaceous sandstone matrix; lenses of soft siltstone, mudstone, and claystone [41]. The Yaifa Formation has been interpreted to have been deposited as fluvial and lake sediments, possibly transitioning to shallow marine, and in part derived from and deposited over earlier volcanics and accumulated locally during periods of volcanic quiescence [41]. The formation is up to 300 m in thickness [41]. The Yaifa Formation was sampled across three separate localities (Table 1; Figures 2–4). Samples 103252 and 103253 are from a highly weathered and degraded outcrop of clay-rich mudstone to sandstone. Samples 103257 and 103258 comprise a mudstone and tuffaceous sandstone, respectively, and represent grain-size variation in a single outcrop adjacent to the Doa Rubber Plantation.

Figure 3. Examples of outcrop sample locations for the Apinaipi Formation, Mt Davidson Volcanics, Yaifa Formation, Astrolabe Agglomerate, and Kore Volcanics. Details of sample locations and rock type descriptions are included in Table 1.

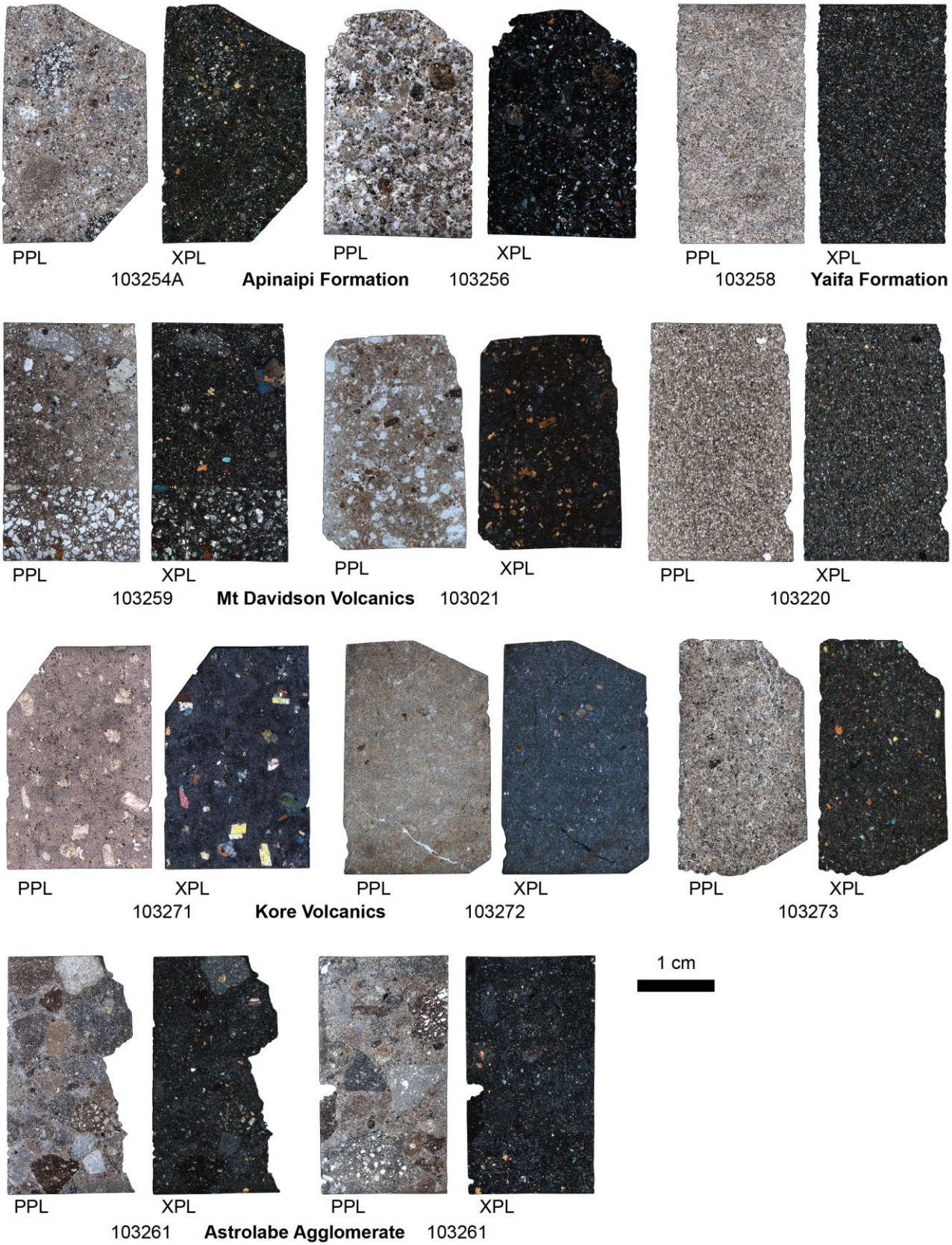

Figure 4. Petrographic mosaic photographs for samples used in this study. For each sample, the image on the left is observed under plane-polarized light, and the right under cross-polarized light. See Table 1 for sample descriptions.

The Pliocene Astrolabe Agglomerate is up to 300 m in thickness and comprises basaltic and minor andesitic laharic agglomerate and tuff with interbeds of volcanically derived conglomerate and sandstone [41]. The Astrolabe Agglomerate is interpreted as nuee ardente-type and airfall pyroclastics and also comprises reworked volcanics in the form of avalanches, lahars, and volcaniclastic sediments in shallow lakes associated with tectonically controlled depressions. No volcanic center has been identified [41]. The Astrolabe Agglomerate was sampled at the Rouna Power Station locality on the margin of the Sogeri Plateau (Figure 2). Sample 103261 comprises a basaltic volcanic agglomerate and represents a bulk sample including both small volcanic clasts and matrix material (Table 1; Figures 3 and 4).

The Mt Davidson Volcanics comprises basaltic and minor andesitic agglomerate, tuff, lava, lava breccia, with intercalated volcanically derived coarse conglomerate and sandstone [41]. The volcanics are up to 600 m in thickness and are interpreted to be deposited during the Pliocene as subaerial volcanics, pyroclastics, and brecciated lava with intercalated laharic and fluvial sediments. No eruptive centers have been identified. Locally, the Mt Davidson Volcanics overlies the Yaifa Formation with a paracomformity, and grades into and is overlain by the Apinaipi Formation [41]. Sampled outcrops of the Mt Davidson Volcanics were isolated and without a context with regard to adjacent rock types. Samples 103021 and 103220 (Table 1; Figures 2–4) are volcaniclastic sandstones, most likely derived from intermediate volcanics. Sample 103259 is a volcanic agglomerate of basaltic to basaltic-andesite derivation.

The Apinaipi Formation is up to 2000 m in thickness and comprises an immature calcareous tuffaceous sandstone, pebble and cobble conglomerate, siltstone, mudstone, minor reefal limestone, volcanic agglomerate, tuff, and brecciated lava [41]. The formation is interpreted to have been deposited predominantly during the Pliocene but extending into the late Miocene, during a period of rapid uplift and volcanism with rapid facies variations from fluvial to deltaic to littoral to shallow-water marine environments. The Apinaipi Formation may be locally derived from, and partly overlies the Mt Davidson Volcanics [41]. Samples 103254A and 103546 (Table 1; Figures 2–4) are from a series of fining upwards packages of tuffaceous clastics on the Mona Highway. Sample 103254A is a bulk sample representative of the matrix and finer clasts within a coarse volcanic conglomerate. Sample 103256 is the finer-grained endmember of the tuffaceous sedimentary package.

4. Methodology

In the laboratory setting, samples were visually screened and washed to remove contamination from attached soil prior to mineral separation. Samples were dried for several days at 100 °C to reduce the moisture content prior to processing. A subset of each sample was prepared for thin section production (Figure 4). The friable and clay-dominated nature of samples from the Yaifa Formation were not amenable to petrographic thin section preparation.

The process of mineral separation to extract zircon crystals followed standard procedures. Initially, samples were crushed and milled to 500 µm. Separation was achieved using a Wilfley table (smaller samples were hand washed to remove the clay fraction) and a combination of heavy liquid density separation and magnetic separation. Zircon crystals were then handpicked without bias towards specific zircon morphologies. The selected zircon crystals were mounted in epoxy and carbon-coated. Cathodoluminescence (CL) images of all zircon crystals used a Jeol JSM5410LV scanning electron microscope equipped with a Robinson CL detector, housed at the Advanced Analytical Centre (AAC), James Cook University (JCU; see Supplementary Material for complete CL images).

All U-Pb dating work was carried out at the AAC, JCU. The dating of zircons was carried out using a Coherent GeolasPro 193 nm ArF Excimer laser ablation system connected to a Bruker 820-ICP-MS. The methodology used for U-Pb dating follows the approach outlined in Holm et al. [42]. The selection of zircon grains for ablation was not biased by their crystal morphology, and all zircons were analyzed with a beam spot diameter of 44 µm.

Some smaller zircon grains were not analyzed due to the spot size, which may incorporate a source of bias into the data. First-cycle volcanogenic zircons that are closest to the eruptive age are likely to be from the smaller populations given the shorter crystallization times during volcanism. The choice of analytical sample spots was guided by CL images.

Data reduction, instrumental drift correction, and analytical processing were performed following the methods described in Holm and Poke [9]. Glitter software (version 4.4.3) was used for data reduction [43]. Drift in instrumental measurements was corrected by analyzing drift trends in the raw data using measured values for the GJ1 primary zircon standard (608.5 ± 0.4 Ma [44]). Secondary zircon standards Temora 2 (416.8 ± 0.3 Ma [45]) and AusZ2 (38.8963 ± 0.0044 Ma [46]) were used to verify GJ1 after drift correction (see Figure A2 in Appendix B).

Age regression and data presentation for all samples were carried out using Isoplot [47]. Corrections for initial Th/U disequilibrium during zircon crystallization, which leads to a deficit of measured ^{206}Pb as a decay product of ^{230}Th [48,49], were applied to all Cenozoic-aged analyses. The corrections were based on Th and U concentrations for zircon determined during LA-ICP-MS analysis, assuming a melt Th/U ratio of 3 ± 0.3 for all zircon analyses due to their reworked nature in secondary deposits. Uncertainties associated with the correction were propagated into errors on the corrected ages following the approach by Crowley et al. [50]. Common Pb was accounted for by visualizing the results on Tera-Wasserburg Concordia plots [44,51]. Spot ages were corrected for common Pb using the Age7Corr algorithms in Isoplot, with the isotopic common-Pb composition modeled from Stacey and Kramers [52].

Isotopic data from detrital and xenocrystic zircon grains were discriminated based on age, following the methodology in Holm and Poke [9]. Grains with ages exceeding 1000 Ma were primarily reported using the ^{207}Pb/^{206}Pb age system, and discordance between the ^{207}Pb/^{206}Pb and ^{206}Pb/^{238}U age systems was assessed. Grains with ages below 1000 Ma were reported based on the ^{206}Pb/^{238}U age system, with evaluation of the discordance between the ^{207}Pb/^{206}Pb and ^{206}Pb/^{238}U, and ^{206}Pb/^{238}U and ^{207}Pb/^{235}U age systems. Analyses with discordance beyond a 20% threshold were excluded from further data reduction. The preferred ages used for analysis were a combination of ^{207}Pb/^{206}Pb and ^{206}Pb/^{238}U ages. All errors were propagated and reported at a 1σ level, unless stated otherwise. A similar methodology was applied to Miocene and younger ages, using a 30% discordance cut-off to account for the increased uncertainty in young U-Pb ages. Additionally, previously published data were used for comparison, with the same discordance criteria applied for consistency (references cited in the associated text and figures). Original datasets were sourced wherever possible for the previously published data.

Maximum depositional ages (MDA) for the samples were calculated via the "youngest three zircons" (Y3Zo) and "youngest single grain" (YSG) methods [53], and the "maximum likelihood age" (MLA [54]). The Y3Zo maximum depositional age was calculated from the weighted average, weighted by date uncertainty, of the youngest three zircons that overlap within a 2σ uncertainty [53,55,56]. The uncertainty of the calculated MDA is the uncertainty of the weighted average. The YSG MDA is the age and uncertainty of the youngest measured grain [55]; the uncertainty is reported as the 95% confidence value. Weighted mean ^{206}Pb/^{238}U age calculations were carried out using Isoplot and reported at 95% confidence. The MLA age was calculated using the radial plot function of IsoplotR [57]. Cumulative probability and histograms were plotted using Isoplot; kernel density estimates (KDE) were plotted according to Vermeesch [58].

Integration of the results from multiple samples simultaneously was carried out using cumulative age distribution (CAD) and multi-dimensional scaling (MDS) plots using IsoplotR [57]. The standard Kolmogorov–Smirnov (KS) statistic is given by the maximum vertical difference between two CAD step functions. The MDS plot of IsoplotR uses the Kolmogorov–Smirnov (KS) statistic coupled with a dimension-reducing technique that takes a matrix of pairwise age dissimilarities between objects as input and produces a 'map'

as output, on which the statistical distance between age distributions of similar samples cluster closely together and dissimilar samples plot far apart [57].

5. Results

The results of the U-Pb zircon dating are compiled from 1050 analyzed zircon grains that yielded 803 concordant ages. Results from the U–Pb zircon dating returned ages ranging from the middle Pliocene up to the Paleoarchean. Of the concordant age data, 221 zircon grains were Cenozoic in age, with 217 of these recording middle Miocene to Pliocene ages. A total of 583 concordant ages were older than the Cenozoic; 46 of these were Cretaceous. These results are presented as two distinct sets of age data. The first comprises the Cenozoic ages, with the majority between middle Miocene and Pliocene age, the youngest age being 4.34 ± 0.13 Ma (1σ error). Most samples yielded Miocene–Pliocene zircon grains; sample 103259 of the Mt Davidson Volcanics, 103261 of the Astrolabe Agglomerate, and samples 103272 and 103273 of the Kore Volcanics did not yield Miocene–Pliocene zircon grains.

The Miocene–Pliocene zircon grains are predominantly euhedral and prismatic with oscillatory zoning (see Supplementary Material), and Th/U ratios ranging from 0.14 to 2.21, with an average of 0.70. These characteristics are consistent with an igneous origin for the Miocene–Pliocene zircons [59–62].

Given the samples that yielded zircon grains for this study are largely sedimentary and volcaniclastic in nature, we will report the maximum depositional ages. As outlined in the previous section, we applied three different methods for reporting the maximum depositional age, the youngest single grain (YSG), the youngest three zircons (Y3Zo), and the maximum likelihood age (MLA). The latter is considered the more statistically robust of the three methods [54], however, Y3Zo age is preferred in this study to represent the most geologically reasonable maximum depositional age, due to the MLA ages incorporating outlying single analytical results that lack a plausible geological justification. In Table 2 and Figure 5, we report the YSG maximum depositional age for each sample and formation, and the Y3Zo and MLA maximum depositional age at the formation level. The maximum depositional age for each formation is considered to be more important on a regional basis as opposed to individual samples that may represent only local depositional ages. Probability–density histograms for the Miocene–Pliocene age results are shown in Figure 5.

The two samples from the Apinaipi Formation yielded YSG ages of 6.53 ± 0.27 Ma (103254A) and 4.34 ± 0.26 Ma (103256) and associated formation maximum depositional ages of 4.52 ± 0.43 Ma (Y3Zo) and 5.08 ± 0.03 Ma (MLA), providing an early Pliocene maximum depositional age for the Apinaipi Formation. Of the four samples derived from the Yaifa Formation, sample 103253 and 103257 returned the oldest YSG ages of 6.38 ± 0.40 Ma and 6.36 ± 0.26 Ma, respectively; sample 102353 yielded a YSG age of 5.81 ± 0.67 Ma, and 103258 provided the youngest YSG age of 5.27 ± 0.80 Ma. The Yaifa Formation yielded a latest Miocene maximum depositional age with a Y3Zo age of 5.8 ± 1.1 Ma and MLA age of 6.76 ± 0.1 Ma. Two of the three samples derived from the Mt Davidson Volcanics yielded latest Miocene–earliest Pliocene YSG ages of 4.59 ± 0.54 Ma (103021) and 5.47 ± 0.81 Ma (103220). An early Pliocene maximum depositional age was calculated for the Mt Davidson Volcanics at 4.66 ± 1.7 Ma (Y3Zo) and 4.97 ± 0.09 Ma (MLA). Sample 103271 of the Kore Volcanics yielded a single concordant Miocene age of 5.64 ± 0.40 Ma; no Y3Zo age was possible for the Kore Volcanics but the MLA yielded a maximum depositional age of 5.66 ± 0.49 Ma.

Table 2. Summary of zircon U-Pb geochronology results.

Formation	Sample	Number of Analyses	Number of Concordant Analyses	Number of Cenozoic Ages	Number of Cretaceous Ages	Number of Ages > Cenozoic	Cenozoic YSG (Ma ± 2σ)	Cenozoic Y3Zo (Ma ± 2σ)	Cenozoic MLA (Ma ± 2σ)	Interpreted Cretaceous Source YSG (Ma ± 2σ)	Interpreted Cretaceous Source Y3Zo (Ma ± 2σ)	Interpreted Cretaceous Source MLA (Ma ± 2σ)
Apinaipi Formation	103254A	91	77	2	10	75	6.53 ± 0.27	-	6.54 ± 0.31	103.5 ± 3.1		
	103256	74	71	70	1	1	4.34 ± 0.26	4.52 ± 0.43	4.78 ± 0.09	100.8 ± 2.9		
	Formation	165	148	72	11	76	4.34 ± 0.26	4.52 ± 0.43	5.08 ± 0.03	100.8 ± 2.9	102.9 ± 5.2	102.3 ± 3.2
Yaifa Formation	103252	100	60	37	3	23	5.81 ± 0.67	6.10 ± 0.35	6.21 ± 0.22	103.9 ± 3.4		
	103253	102	61	31	8	30	6.38 ± 0.40	6.59 ± 0.19	6.73 ± 0.12	96.9 ± 3.4		
	103257	65	51	1	2	50	6.36 ± 0.26	-	-	105.8 ± 3.4		
	103258	55	36	7	0	29	5.27 ± 0.80	7.81 ± 0.31	5.70 ± 0.84	-		
	Formation	322	208	76	13	132	5.27 ± 0.80	5.8 ± 1.1	6.76 ± 0.1	96.9 ± 3.4	103.1 ± 6.8	98.0 ± 5.5
Mt Davidson Volcanics	103021	100	71	42	2	29	4.59 ± 0.54	4.66 ± 0.18	4.84 ± 0.19	96.7 ± 3.1		
	103220	91	48	29	5	19	5.47 ± 0.81	5.79 ± 0.22	6.00 ± 0.14	76.5 ± 2.5		
	103259	86	72	0	0	72	-	-	-	-		
	Formation	277	191	71	7	120	4.59 ± 0.54	4.66 ± 1.7	4.97 ± 0.09	76.5 ± 2.5	-	76.95 ± 3.7
Astrolabe Agglomerate	103261	55	53	1	6	52	36.9 ± 1.7	-	37.0 ± 2.2	98.1 ± 2.8	99.9 ± 1.5	99.8 ± 1.8
Kore Volcanics	103271	55	49	1	2	48	5.64 ± 0.40	-	5.66 ± 0.49	101.2 ± 2.9		
	103272	76	72	0	7	72	-	-	-	96.4 ± 2.8		
	103273	100	82	0	0	82	-	-	-	-		
	Formation	231	203	1	9	202	5.64 ± 0.40	-	5.66 ± 0.49	96.4 ± 2.8	103.5 ± 5.6	97.6 ± 3.7
Total		1050	803	221	46	582						

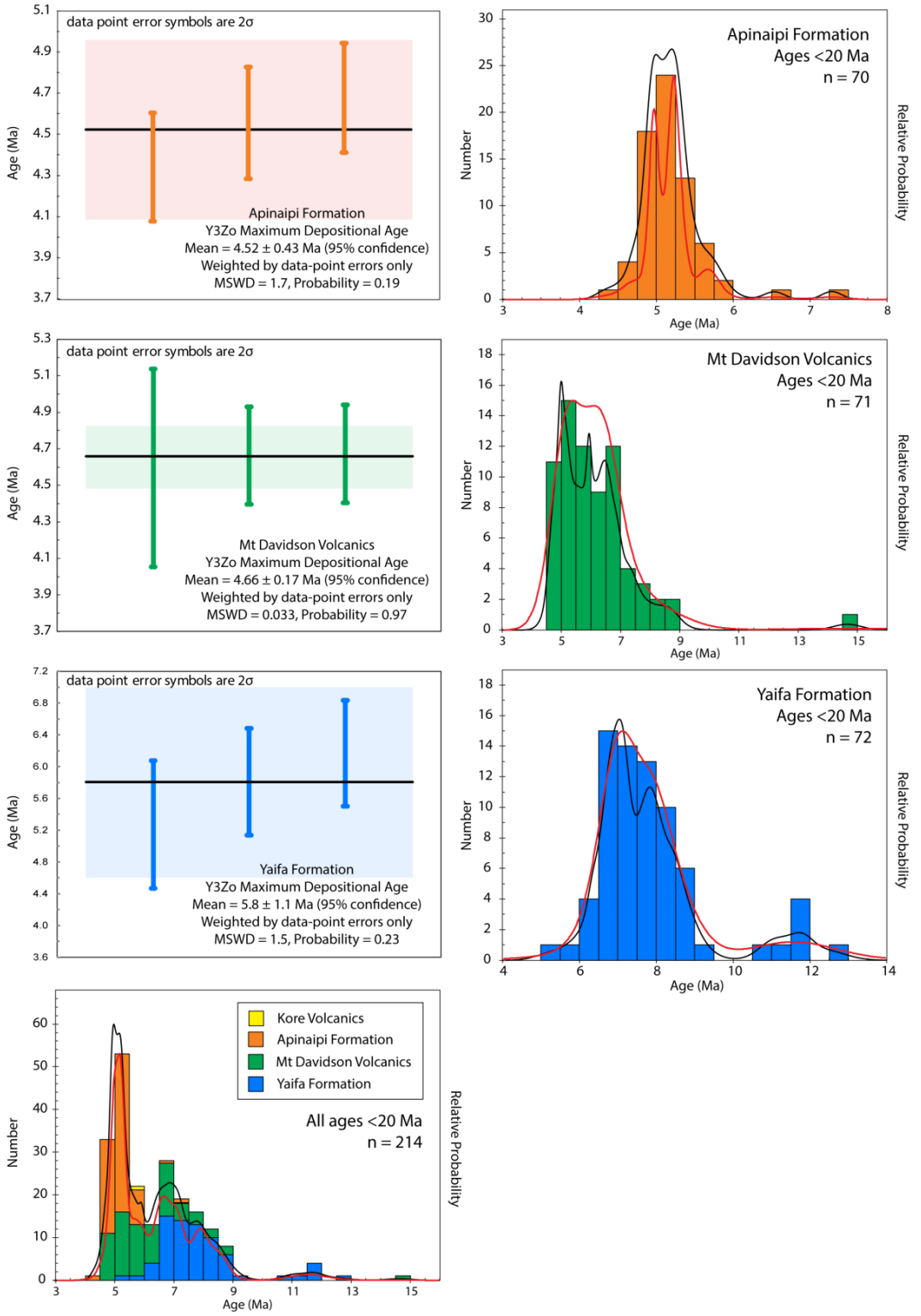

Figure 5. Zircon U–Pb dating results for the Miocene–Pliocene resultant ages of the Apinaipi Formation, Mt Davidson Volcanics, and Yaifa Formation; see Table 2 for summary results; Kore Volcanics and Astrolabe Agglomerate yielded insufficient Miocene–Pliocene U-Pb ages to interpret weighted average ages. Weighted average Y3Zo plots are constructed from zircon U–Pb-calculated ages corrected for initial Th disequilibrium and $^{207}Pb/^{206}Pb$ common Pb (detailed isotopic data in Supplementary Material). Probability–density histograms and KDE (red lines) are shown for the Apinaipi Formation, Mt Davidson Volcanics, Yaifa Formation, and a summary plot including results from the Kore Volcanics.

Although the rocks investigated for this study are Miocene–Pliocene in age, the majority of zircons analyzed were inherited grains with 582 concordant zircon analyses dated as Cretaceous to Paleoarchean in age. The distribution of age populations between individual samples and formations do not vary significantly (Figure 6); this will be explored further below. Here, we report on the compiled results for the ages of inherited zircon grains for all samples combined; results for individual samples are available in the Supplementary Material. In this study, the term inherited is defined as all zircon grains derived from an older source and includes both xenocrystic and detrital zircon grains. Within the inherited grains of Cretaceous and older ages, significant age populations within the dataset include a Cretaceous population (46 grains [8%]) that peaks at ca. 100 Ma; a Carboniferous–Triassic (ca. 359–201 Ma) population that comprises just 20 grains (3%); a Devonian–Silurian (ca. 444–359 Ma) population of 42 grains (7%); 65 grains of Ordovician age (ca. 485–444 Ma; 11%) with a peak at ca. 470–460 Ma; 39 Cambrian grains (ca. 541–485 Ma; 7%); 60 Ediacaran grains (ca. 635–541 Ma; 10%); 74 Tonian–Cryogenian grains (1000–635 Ma; 13%) with relative peaks at ca. 690 Ma and ca. 950 Ma; 65 grains of Stenian age (1200–1000 Ma; 11%), peaking broadly between ca. 1200 and 1100 Ma; 60 Calymmian–Ectasian grains (1600–1200 Ma; 10%); 72 Paleoproterozoic grains (2500–1600 Ma; 12%) with a peak at ca. 1650 Ma; and 35 grains of middle Paleoarchean to Paleoproterozoic age (3400–2500 Ma; 6%).

Given the prevalence and importance of the Cretaceous-aged zircons in this study, and from similar previous studies of the Papuan Peninsula [8,9,21,22], we also report interpreted Cretaceous depositional ages for samples analyzed during this study (Table 2; Figure 7).

The approach to calculating the Cretaceous YSG, Y3Zo, and MLA depositional ages utilized the same methods as those for Cenozoic ages outlined above. The results presented here will be explored in further detail in the discussion. Samples 103254A and 103256 from the Apinaipi Formation yielded Cretaceous YSG ages of 103.5 ± 3.1 Ma and 100.8 ± 2.9 Ma, respectively, with associated Cretaceous ages of 102.9 ± 5.2 Ma (Y3Zo) and 102.3 ± 3.2 Ma (MLA). Three of the four samples derived from the Yaifa Formation yielded Cretaceous ages with samples 103252, 103253 and 103257 returning the YSG ages of 103.9 ± 3.4 Ma, 96.9 ± 3.4 Ma and 105.8 ± 3.4 Ma, respectively. The Yaifa Formation yielded Cretaceous ages of 103.1 ± 6.8 Ma (Y3Zo) and 98.0 ± 5.5 Ma (MLA). Sample 103259 of the Mt Davidson Volcanics did not yield any Cretaceous ages; the remaining two samples yielded Cretaceous YSG ages of 96.7 ± 3.1 Ma (103021) and 76.5 ± 2.5 Ma (103220). It was not possible to calculate a Y3Zo age, however, the MLA returned an age of 76.95 ± 3.7 Ma. The Astrolabe Agglomerate yielded sufficient Cretaceous zircon ages with a YSG age of 98.1 ± 2.8 Ma, a Y3Zo age of 99.9 ± 1.5 Ma, and an MLA age of 99.8 ± 1.8 Ma. Samples 103271 and 103272 of the Kore Volcanics returned Cretaceous YSG ages of 101.2 ± 2.9 Ma and 96.4 ± 2.8 Ma, respectively; sample 103273 did not yield any Cretaceous zircon grains. A Cretaceous Y3Zo age of 103.5 ± 5.6 Ma and an MLA age of 97.6 ± 3.7 Ma was calculated for the Kore Volcanics. The middle Cretaceous Y3Zo age results are consistent with previous studies of the Owen Stanley Metamorphic Complex based on U-Pb dating of zircon and preserved macrofossils [8,21,22].

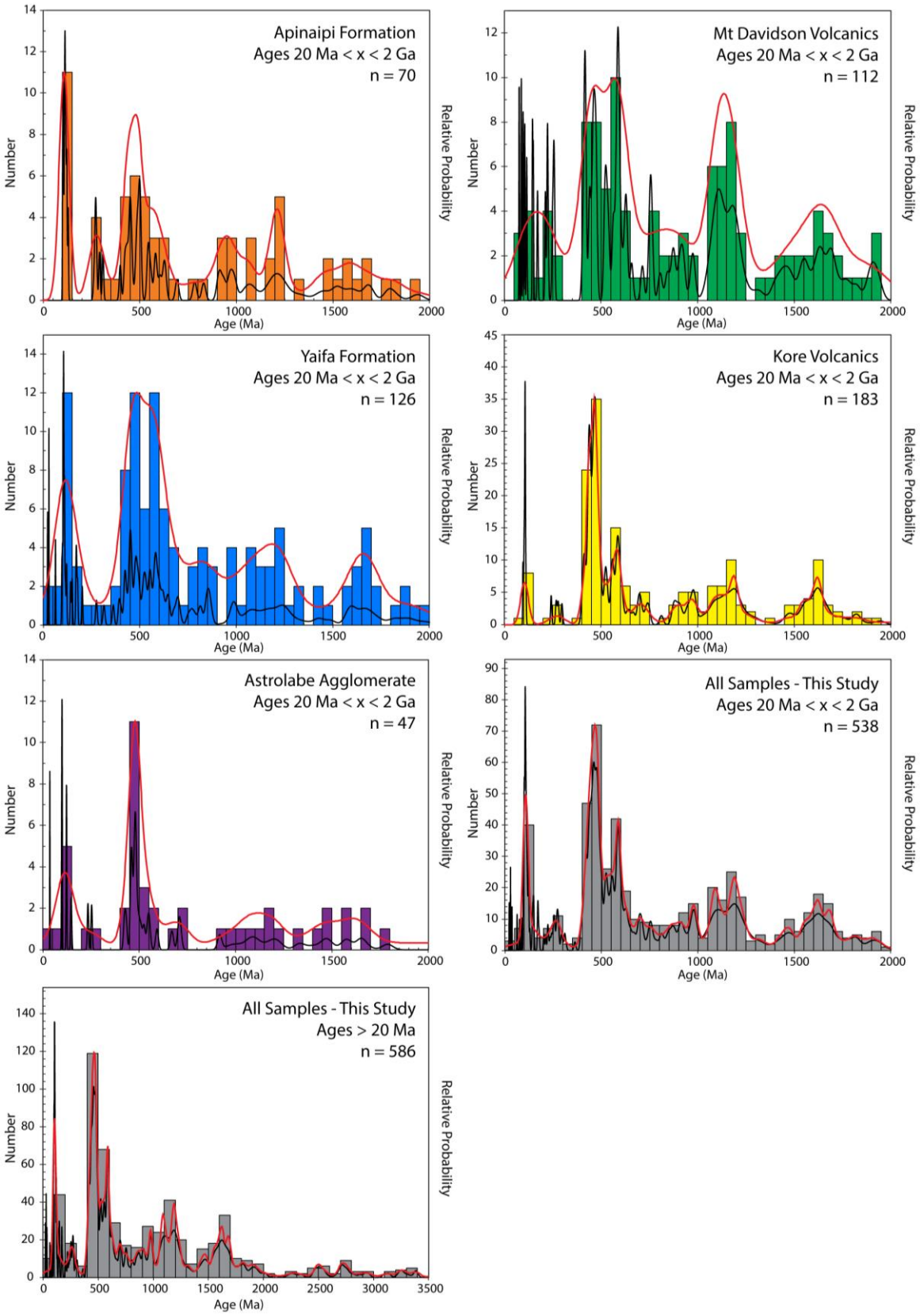

Figure 6. Probability–density histograms and KDE (red lines) are shown for U–Pb dating results of inherited zircon grains. Plots are presented for the Apinaipi Formation, Mt Davidson Volcanics, Yaifa Formation, Kore Volcanics, Astrolabe Agglomerate, and summary plots of aggregated U-Pb dating results for all samples in this study.

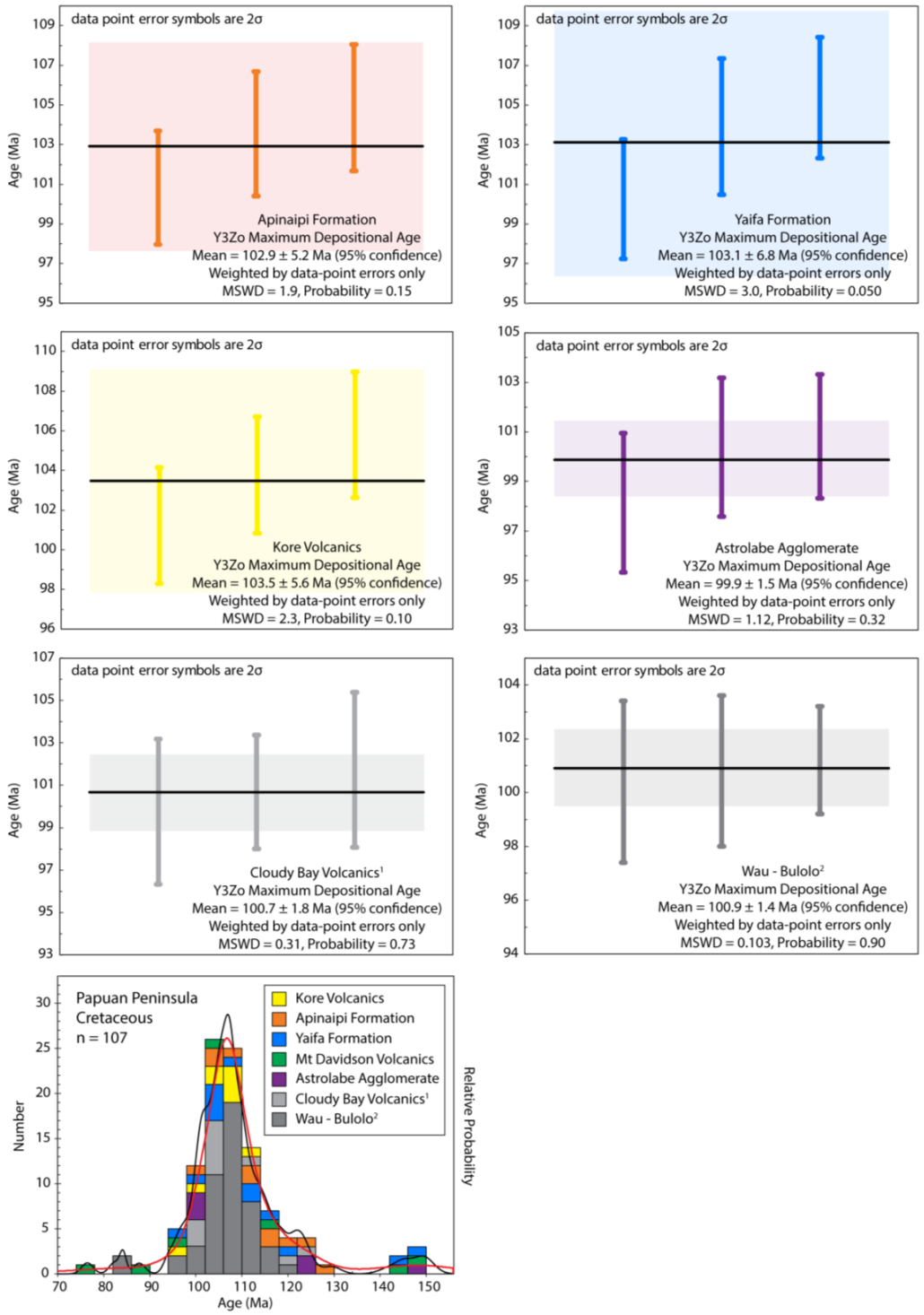

Figure 7. Zircon U–Pb dating results for inherited Cretaceous zircon grains of the Apinaipi Formation, Yaifa Formation, and Kore Volcanics; see Table 2 for summary results. Weighted average Y3Zo plots are constructed from zircon U–Pb calculated ages corrected for initial Th disequilibrium and $^{207}Pb/^{206}Pb$ common Pb (detailed isotopic data in Supplementary Material). Similar plots were constructed for comparison of the (1) Cloudy Bay Volcanics [9] and (2) metasediments of Wau-Bulolo [8]. The Mt Davidson Volcanics yielded insufficient Cretaceous U-Pb ages. A probability–density histogram and KDE (red line) is shown for the aggregated Cretaceous ages of the Apinaipi Formation, Mt Davidson Volcanics, Yaifa Formation, Kore Volcancis, Astrolabe Agglomerate, and the cited sample suites from the Cloudy Bay Volcanics and Wau-Bulolo area.

6. Discussion

6.1. Miocene–Pliocene Volcanism and Sedimentation

The detrital composition of volcaniclastics in this study (e.g., Apinaipi Formation, Yaifa Formation and Mt Davidson Volcanics) are dominated by quartz-poor clastic rocks that were derived from a nearby volcanic source, and volcanic–lithic detritus dominates the lithic component. Some of the volcaniclastic rocks contain detrital pyroxene or amphibole, confirming their first cycle and immature nature. The presence of feldspar in many of the samples is interpreted to represent first-cycle volcanics and crystal tuffs that may have undergone some reworking by fluvial systems. The immature nature of the volcaniclastic rocks sampled is also consistent with the presence of the primary volcanics, volcanic agglomerates, and volcanic conglomerates (e.g., Kore Volcanics, Astrolabe Agglomerate, and Mt Davidson Volcanics).

Samples of basaltic volcanics and volcaniclastic sediments of basaltic derivation did not yield any Miocene–Pliocene zircon grains; this included sample 103259 of the Mt Davidson Volcanics, the Astrolabe Agglomerate, and samples 103272 and 103273 of the Kore Volcanics. Sample 103271, a basaltic-andesite from the Kore Volcanics yielded only a single zircon with an analyzed Miocene–Pliocene U-Pb age. In contrast, volcaniclastics of the Apinaipi Formation, samples 103021 and 103220 of the Mt Davidson Volcanics, and samples from the Yaifa Formation generally returned more abundant Miocene–Pliocene U-Pb zircon ages. This result is not surprising considering these latter volcanic and volcaniclastic formations are derived from compositionally more intermediate volcanism where the source magma had likely undergone sufficient fractionation to allow the crystallization of zircon.

The U-Pb zircon dating carried out as part of this study provides new constraints for the timing of activity of the Kore Volcanics and magmatism that contributed material to the volcaniclastic Apinaipi Formation, Mt Davidson Volcanics, and Yaifa Formation along the southern Papuan Peninsula. Zircon U–Pb dating results indicate that magmatic activity, with sufficiently fractionated magma to fractionate zircon, was primarily constrained to the late Miocene–early Pliocene along the southern Papuan Peninsula, and between ca. 9 and 4.5 Ma in age. However, the zircon record extends back to ca. 12 Ma, and even ca. 15 Ma if minor zircon age populations are taken into consideration. This age range does not account for zircon crystallization post-dating the deposition of the volcanics and volcaniclastics that were sampled as part of this work.

Deposition of the Yaifa Formation and Kore Volcanics is constrained by Messinian maximum depositional ages. These ages correlate with the mapped age of the Yaifa Formation and Kore Volcanics as late Miocene–early Pliocene and Miocene, respectively. The dating results for the Kore Volcanics, however, are not considered conclusive, with only one concordant Messinian age and several additional discordant Tortonian ages. The Kore Volcanics sampled during this study are interpreted to have been deposited as subaerial and shallow marine volcanics and pyroclastics, whereas the Yaifa Formation represents deposition during periods of volcanic quiescence in fluvial and lake sediments, possibly shallow marine in part [41].

The timing for deposition of the Mt Davidson Volcanics and Apinaipi Formation are well constrained by Zanclean maximum depositional ages, in agreement with the mapped Pliocene age of both formations. Deposition of the Mt Davidson Volcanics and Apinaipi Formation during the Zanclean is interpreted to coincide with a period of uplift and volcanism with rapid facies variations, represented in outcrop by the large range of grain size and sorting characteristics. No eruptive centers have been linked with the Mt Davidson Volcanics or Apinaipi Formation [41].

The Astrolabe Agglomerate failed to yield any concordant Miocene or Pliocene analyses but has been mapped as being of Pliocene age. No identified volcanic center has been linked to the Astrolabe Agglomerate, which is interpreted as nuee ardente-type and airfall pyroclastics, and reworked volcanics in avalanches, lahars, and volcaniclastic sediments [41].

The range of ages from the U-Pb analyses of ca. 15 Ma to 4.5 Ma encompasses the range of volcanism known from the southern Papuan Peninsula. Older magmatic events within this age range are recorded by, for example, the Fife Bay Volcanics dated at 12.6 Ma [23,33]; high-K basalts of Woodlark Island dated at 11.2 Ma [33,63]; and plutons and dyke swarms that intrude the eastern Milne Basic Complex, and dated at 16–12 Ma [30,33]. More recent regional volcanism within the U-Pb dating range comprises andesites and shoshonites north of and adjacent to the D'Entrecasteaux islands, dated at 5.5 Ma, a granite intrusive complex at Mt Suckling dated at 6.3 Ma [23,33], and the Cloudy Bay Volcanics dated at between ca. 7 and 5 Ma in age [9]. This latter volcanism marked a transition from early submarine–subaerial activity to entirely subaerial volcanism during the Pliocene and Quaternary, reflecting the emergence of eastern Papua New Guinea [5].

6.2. Origin of the Inherited Zircons

The majority of zircon grains analyzed from the sampled Miocene–Pliocene volcanics and volcaniclastics are of pre-Cenozoic age (78% of concordant analyses; Table 2; Figure 6), and represent xenocrystic or detrital zircon grains inherited from a foreign source. Such inherited zircons have also been found in recent studies from the Papuan Peninsula. Osterle et al. [24] investigated samples from the Bonenau Schist, intercalated within the Goropu Metabasalt (youngest concordant subpopulation ages of 103.3 ± 2.7/4.9 Ma and 71.8 ± 1.1/3.1 Ma), the Suckling Granite (3.7 ± 0.03/0.2 to 3.3 ± 0.05/0.1 Ma), Mai'iu Monzonite (2.9 ± 0.12/0.2 to 2.0 ± 0.08/0.1 Ma), and the Bounua Porphyry (3.4 ± 0.07/0.2 Ma). The study found extensive zircon inheritance dating back to at least the Paleoproterozoic, but with common Cretaceous age peaks. The Bonenau Schist returned age peaks of ca. 103 and 71 Ma, whereas the Suckling Granite, Mai'lu Monzonite, and the Bonua Porphyry all yielded age peaks of ca. 100 Ma [24]).

Holm and Poke [9] found similar results in a study of the Cloudy Bay Volcanics of the southeast Papuan Peninsula, where the ca. 7–5 Ma aged volcanics contained a high proportion of inherited zircons dating back to the Mesoarchean. The study of Holm and Poke [9] also found a significant population of euhedral and prismatic zircon grains with a broad ca. 120–100 Ma Cretaceous age range. The origin of these Cretaceous and older inherited zircons was interpreted to be the regionally extensive Owen Stanley Metamorphic Complex with an Albian–Cenomanian depositional age [9,21,22]. This does not preclude the existence of an older continental basement beneath the Owen Stanely Metamorphic Complex, however, there is currently no direct evidence for such older crust [3,5,8,21,23]. Holm and Poke [9] also noted that the abraded and rounded morphology of the majority of pre-Cretaceous zircon grains indicated they were detrital in origin and may not have originated from the Papuan Peninsula.

Results of the U-Pb zircon dating in this study yielded similar inherited zircon ages. Four of the five Miocene–Pliocene volcaniclastic formations selected for this study yielded sufficient Cretaceous zircon to derive Y3Zo ages (Table 2; Figure 7). Three of these formations, the Apinaipi Formation, Yaifa Formation, and Kore Volcanics, yielded maximum depositional Albian Y3Zo ages of ca. 103 Ma; the Astrolabe Agglomerate yielded a maximum depositional Cenomanian Y3Zo age of ca. 100 Ma.

Figure 8 utilizes the CAD and MDS plots described above as a measure of similarity or dissimilarity to compare the sample suite of this study to other detrital zircon studies from the wider Papuan Peninsula. The potential source areas for comparison include results from Wau-Bulolo, Morobe [8,64], and Cloudy Bay, eastern Papuan Peninsula [9]. Although this is still a relatively small dataset, the interpreted similarity of zircon inheritance within the Miocene–Pliocene samples is indicated by clustering of the data points, compared with the more dissimilar Wau-Bulolo sample points. This demonstrates that the parent Cretaceous volcaniclastic rocks, from which the Miocene–Pliocene rocks in this study were derived, were likely deposited at a similar time with derivation from a common source at the regional scale.

The maximum depositional ages interpreted in this study are similar to the Albian–Cenomanian maximum depositional ages found for the Goropu Metabasalt [24] and basement ages inherited within the Cloudy Bay Volcanics [9], indicating the samples utilized in this study were most likely derived from a similar basement protolith at the regional scale; the source for zircon inheritance in this study, either through xenocrystic or detrital origins, is interpreted as the Owen Stanley Metamorphics. The middle Cretaceous maximum depositional age appears to be widespread across the Papuan Peninsula and is likely of regional significance for the basement rocks. The context and source for the spectrum of zircon inheritance in the Owen Stanley Metamorphics will be interpreted in the next section.

6.3. Regional Zircon Provenance

The majority of zircon grains recovered from the sampled volcanics and volcaniclastics are of pre-Cenozoic age and represent inherited zircon grains from a foreign source. Within the inherited grains, significant age populations comprise Cretaceous ages as outlined above, and also Carboniferous–Triassic ages (ca. 359–201 Ma), Devonian–Silurian ages (ca. 444–359 Ma), Ordovician ages (ca. 485–444 Ma), Cambrian ages (ca. 541–485 Ma), Ediacaran ages (ca. 635–541 Ma), Tonian–Cryogenian ages (1000–635 Ma) with relative peaks at ca. 690 Ma and ca. 950 Ma, Stenian age (1200–1000 Ma), peaking broadly between ca. 1200 and 1100 Ma, Calymmian–Ectasian grains (1600–1200 Ma), Paleoproterozoic grains (2500–1600 Ma) with a peak at ca. 1650 Ma, and a broad range of middle Paleoarchean to Paleoproterozoic ages (3400–2500 Ma). Figures 7 and 8 demonstrate that the parental Cretaceous volcaniclastic rocks, from which the zircon grains in the Miocene–Pliocene rocks in this study were interpreted to be derived, were likely deposited at ca. 100 Ma, with derivation from a similar or common source at the regional scale.

Here, we discuss the potential sources for the zircon inheritance, and by association, the wider tectonic and depositional context of the parental Cretaceous basement underlying the Papuan Peninsula. To achieve this, we compare the results from this study with previous studies of regional late Mesozoic rocks and potential sediment sources of northeastern Australia and the Southwest Pacific, and utilize qualitative age distribution assessments and the MDS plot described above as a measure of the similarity and dissimilarity. The areas for comparison include lower to middle Permian and Cretaceous rocks of the Wau-Bulolo region, Morobe—northwest Papuan Peninsula [8,64]; Miocene–Pliocene Cloudy Bay Volcanics, eastern Papuan Peninsula [9]; eastern New Guinea Highlands, upper Permian to Early Triassic Omung Metamorphics and Goroka Formation, and Upper Triassic Bena Bena Formation [7]; (the Goroka and Bena Bena Formations are combined on the basis of spatial proximity and age spectra similarity); Far North Queensland basement inliers, late Mesoproterozoic Iron Range Province [65], and Proterozoic Georgetown Inlier [66]; Northeast Queensland basement inliers, Silurian and Devonian Mossman Orogen, and late Neoproterozoic to Cambrian Charters Towers Block and Anakie Inlier [67]; North Queensland inland Mesozoic basins, Northern Eromanga Basin, Lower and Middle Jurassic Hutton Sandstone, and Blantyre Sandstone [68], and middle Cretaceous Winton Formation and Makunda Formation [69]; Central Queensland coastal Mesozoic basins, middle Carboniferous Shoalwater Formation and Beenleigh Block [70]; upper Carboniferous to lower Permian rocks of the Queensland Plateau [71]; and rocks of New Caledonia ranging in age from Permian to Upper Triassic [72] and Upper Cretaceous to lowermost Eocene [73].

Figure 9 presents CAD and MDS plots to illustrate the similarity and dissimilarity of samples in this study to regional late Mesozoic rocks and potential sediment sources of northeastern Australia for different age ranges. Results from this study are plotted according to the geological formation or unit, as well as an inclusive population representing all results from this study together with results from Cloudy Bay (eastern Papuan Peninsula [9]) on the basis of similarity in Figure 8. Over the full age spectrum (Cretaceous and older ages; Figure 9A,B) the inherited zircon ages of this study are most similar to age spectra from the Queensland Plateau, and the Beenleigh Block and Shoalwater Formation of the central Queensland coastal area. Age populations from basement inliers of Northeast

Queensland (Charters Towers Block, Anakie Inlier and Mossman Orogen) plot in a broad cluster; age populations from New Caledonia, the Winton, and Makunda Formations, and populations from the eastern New Guinea Highlands and northwest Papuan Peninsula (Wau-Bulolo, Goroka and Bena Bena Formations, and Omung Metamorphics), similarly form a broad cluster, indicating a degree of similarly. This comparison, although useful at the broadest scale, is affected by inherent biases in the range of younger ages, derived from the differences in depositional ages. For example, Iron Range represents an older basement inlier that lacks younger age components and plots distal or dissimilar to other sample populations as a result. By subdividing the evaluated age ranges into older Precambrian basement age generations (e.g., ages > ca. 400 Ma; Figure 9C,D) and younger ages spanning the convergent margin history of the eastern Australia Tasmanide Orogen (approximately the Cambrian to the Hunter Bowen Orogeny, ca. 230 Ma [67,74]; Figure 9E,F), we can better understand the implications for similarities and differences in regional-scale zircon provenance.

Older inheritance ages (ca. > 400 Ma) are representative of potential basement provenance that may include both primary and secondary recycling of zircon grains from their original source (Figure 9C,D). Most zircon age spectra used in this study demonstrate a marked similarity in older age inheritance with a large cluster encompassing the majority of sample sets, including samples from the Papuan Peninsula. Two end-member basement populations illustrate potential distinct sources; these are the Iron Range and Georgetown Inlier of Far North Queensland, and the Charters Towers Block and Anakie Inlier of North Queensland. It is worth noting that the Omung Metamorphics and Goroka and Bena Bena Formations of the eastern New Guinea Highlands plot adjacent to the basement inliers of Far North Queensland, consistent with the interpretation of Van Wyck and Williams [7], which may imply derivation of basement grains from a common provenance or recycling of these basement rocks through multiple phases of deposition and erosion. The main sample cluster, including the Papuan Peninsula, represents a distinct population with either a different or mixed basement provenance.

The largest diversity in age spectra is evident within the age range spanning activity of the Tasmanides of eastern Australia (Figure 9E,F; Cambrian to the Hunter-Bowen Orogeny, ca. 230 Ma). This range in evaluated ages excludes basement inliers with a significantly older depositional age and zircon inheritance that may have undergone multiple phases of recycling, and therefore may be distal from its original source. Instead, this age range highlights likely primary and proximal provenance regions and adjacent depositional basins. Interestingly, Figure 9E,F indicate that the Papuan Peninsula shares a similar inheritance age spectrum with the Central Queensland Mesozoic basins (Beenleigh Block and Shoalwater Formation) and New Caledonia, but is quite dissimilar to the Far North and North Queensland sample populations. Samples from Wau-Bulolo and eastern New Guinea Highlands are most similar to the North Queensland Mesozoic basins and New Caledonia and are again dissimilar to the Georgetown Inlier population that represents Far North Queensland.

This comparison of age spectrum similarity provides consistent results, where zircon age inheritance of the Papuan Peninsula is not compatible with potential source regions of North and Far North Queensland, in that they lack significant late Paleozoic and early Mesozoic age populations, and are instead more similar to the Central Queensland Beenleigh Block, Shoalwater Formation, and New Caledonia. The Papuan Peninsula and Shoalwater Formation zircon age spectra share Ediacaran to Silurian (ca. 650–420 Ma), middle Mesoproterozoic to early Neoproterozoic (ca. 1250–950 Ma), and late Paleoproterozoic (ca. 1700–1550 Ma) age peaks, and in both sample sets the Carboniferous–Permian zircon population that is characteristic of the North Queensland Kennedy Igneous Association (330–270 Ma [75]) are notably absent. Previous tectonic reconstructions [3,5,10,12,14] indicate that the Papuan Peninsula was positioned next to Far North Queensland at ca. 100 Ma. However, these models need to be questioned in light of the detrital zircon age data presented here. The age populations of zircon derived from the basement of the Papuan Peninsula are interpreted to have originated further south, adjacent to the Central Queensland margin (Figure 10). These findings provide a robust evidence-based provenance

model that confirms that many of the terranes are allochthonous in nature and indicates that existing tectonic reconstructions require major revision.

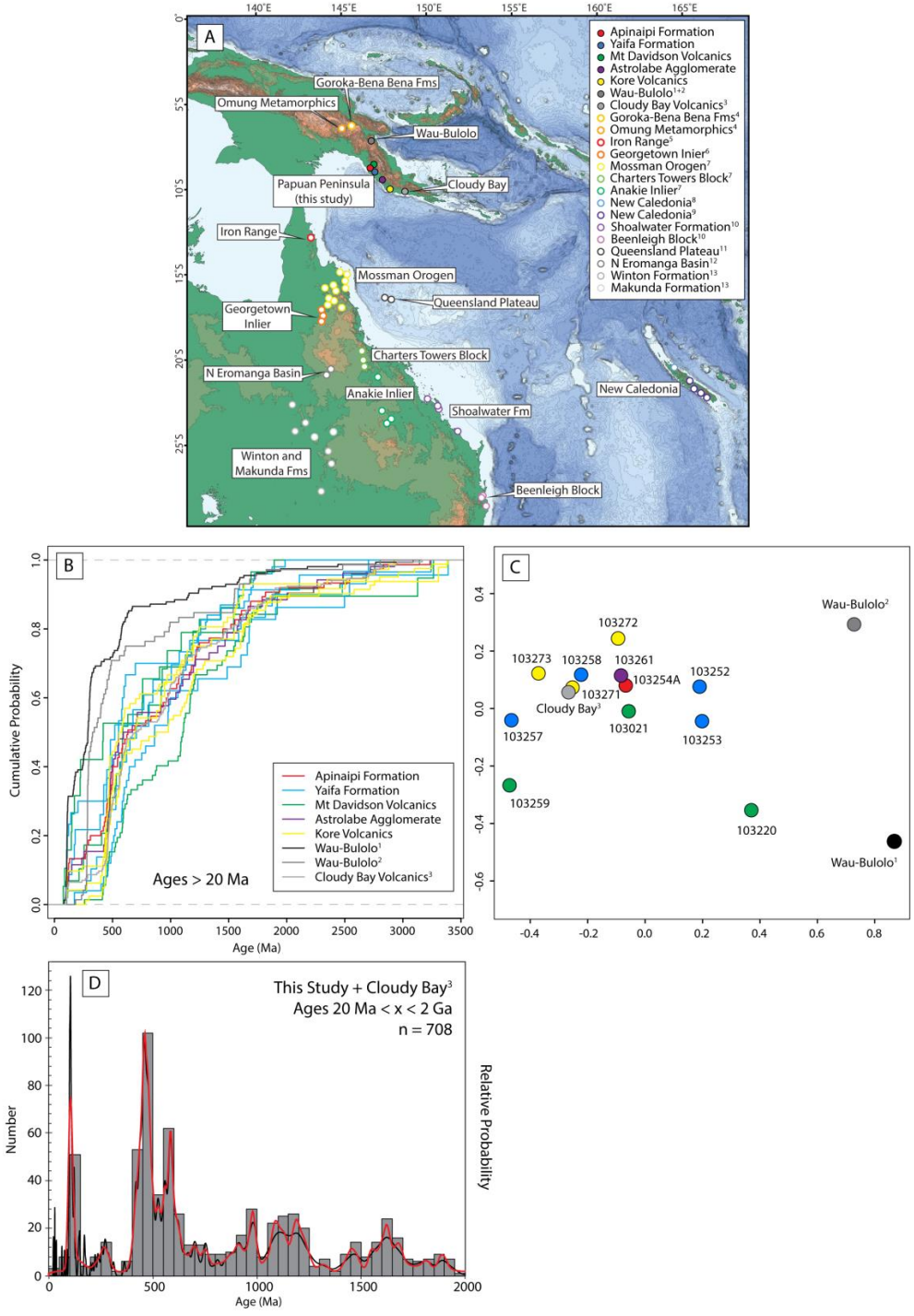

Figure 8. (**A**) Locations for sample suites used for comparison for discussion. References for samples suites: (1) Kopi et al. [8]; (2) Bodorkos et al. [64]; (3) Holm and Poke [9]; (4) Van Wyck and Williams [7]; (5) Blewett et al. [65]; (6) Murgulov et al. [66]; (7) Shaanan et al. [67]; (8) Pirard and Spandler [73]; (9) Campbell et al. [72]; (10) Korsch et al. [70]; (11) Shaanan et al. [71]; (12) Cheng et al. [68]; (13) Tucker et al. [69]. (**B**,**C**) CAD and MDE plots for comparison of inherited zircon grains sampled from the Papuan Peninsula, including Wau-Bulolo and the Cloudy Bay Volcanics. (**D**) Probability–density histogram and KDE (red line) correlating and aggregating results from this study and the Cloudy Bay Volcanics into a compiled southeast Papuan Peninsula sample suite.

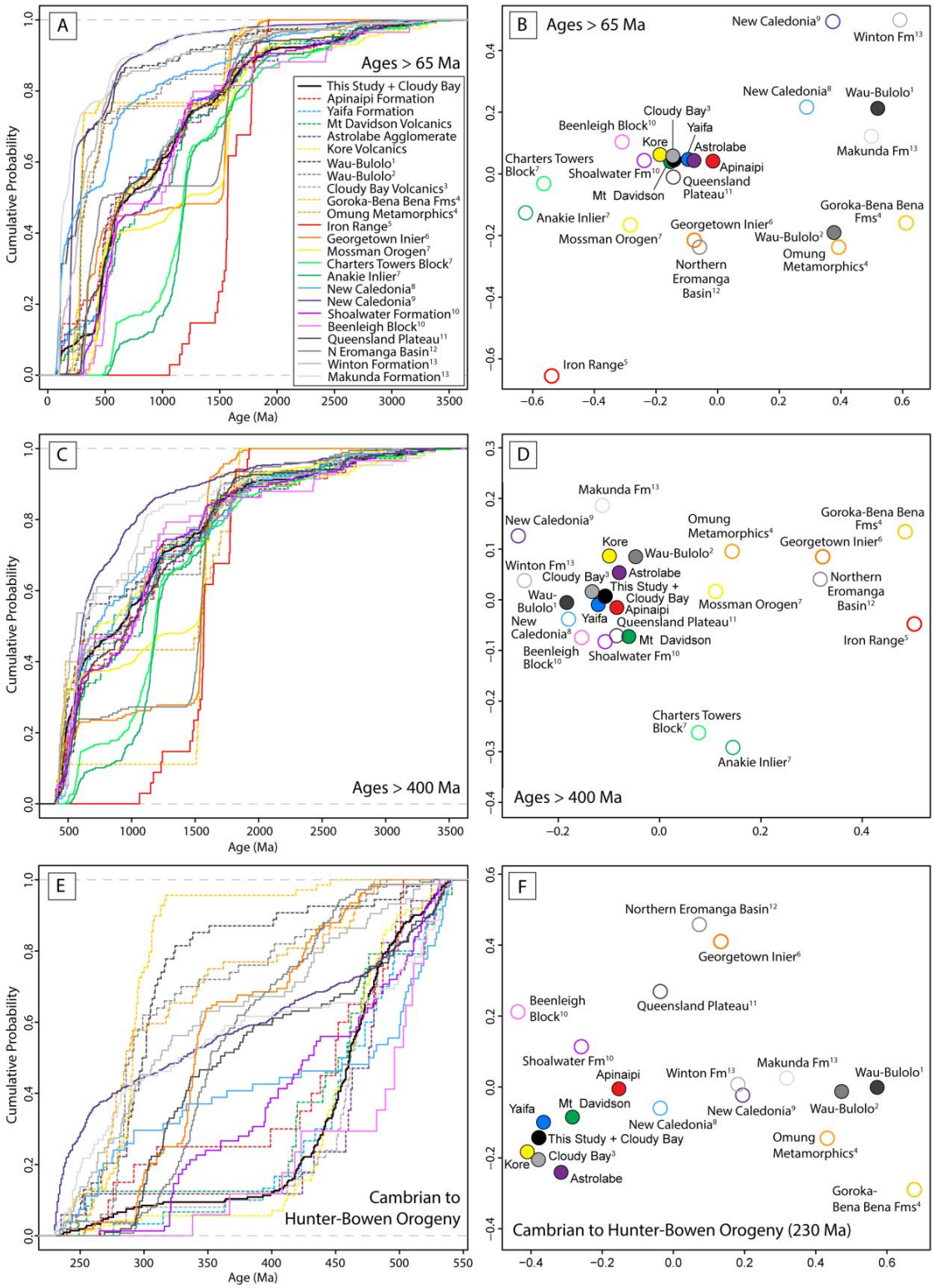

Figure 9. Regional Southwest Pacific and eastern Australia MDE and CAD plots for selected age ranges (see text for discussion). A and B includes all ages less than 65 Ma; C and D include all ages less than 400 Ma; E and F includes between the Cambrian and Hunter Bowen Orogeny at 230 Ma. Location of samples is shown in Figure 8. References for samples suites: (1) Kopi et al. [8]; (2) Bodorkos et al. [64]; (3) Holm and Poke [9]; (4) Van Wyck and Williams [7]; (5) Blewett et al. [65]; (6) Murgulov et al. [66]; (7) Shaanan et al. [67]; (8) Pirard and Spandler [73]; (9) Campbell et al. [72]; (10) Korsch et al. [70]; (11) Shaanan et al. [71]; (12) Cheng et al. [68]; (13) Tucker et al. [69].

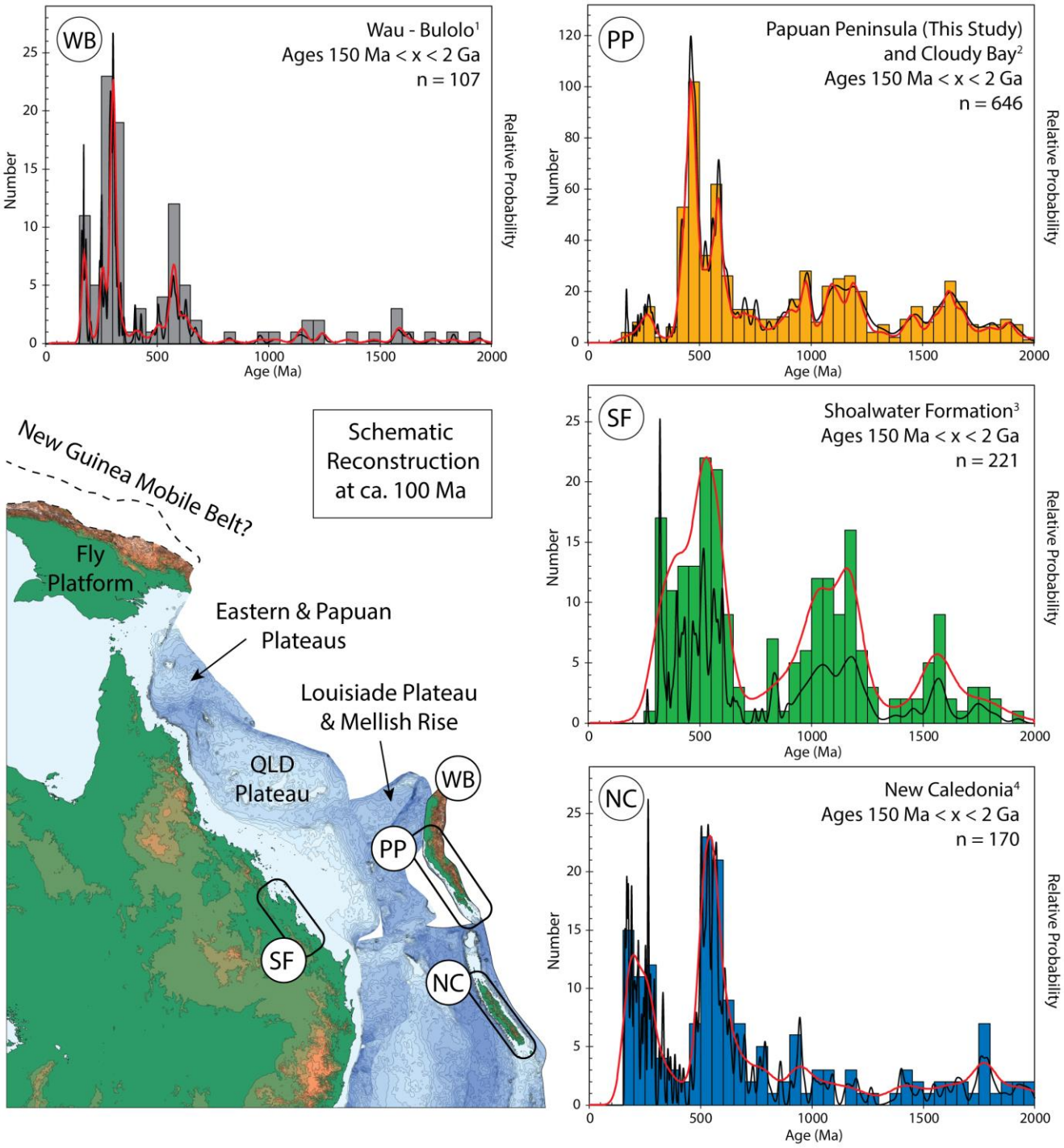

Figure 10. Schematic reconstruction for the location of the Papuan Peninsula depocenter at ca. 100 Ma. The schematic reconstruction was modified from Matthews et al. [76] utilizing GPlates 2.0 software [77]. Comparative probability–density histograms and KDE (red lines) are shown for Wau-Bulolo (1: Kopi et al. [8]), the compiled southeast Papuan Peninsula including samples from this study and the Cloudy Bay Volcanics (2: Holm and Poke [9]), the middle Carboniferous Shoalwater Formation of the Central Queensland margin (3: Korsch et al. [70]), and Upper Cretaceous to lowermost Eocene rocks of New Caledonia (4: Pirard and Spandler [73]). See text for discussion.

6.4. Implications for Regional Tectonics

The findings above are supported by previous work; for example, Little et al. [78] and Osterle et al. [24] have previously noted that the Papuan Peninsula and New Caledonia

share striking similarities with regard to their tectonic history. The similarities include a tectonic and crustal framework for emplacement of ophiolitic rocks over an allochthon comprising mostly Late Cretaceous marginal basin rocks of MORB-affinity (Poya Terrane in New Caledonia; Goropu-Kutu in PNG). Additionally, paleomagnetic data of Klootwijk et al. [79] support an interpretation that northern New Guinea had a more southerly palaeolatitude compared to southern New Guinea prior to the Paleogene [80]. Further afield, Decker et al. [81] and Webb et al. [82] have interpreted that age populations of zircons recorded from Jurassic–Cretaceous sedimentary sequences from the Tamrau Formation of the Bird's Head, West Papua–Indonesia, and the Lengguru Fold and Thrust Belt of the Bird's Neck are unlikely to have been derived from adjacent Palaeozoic basement rocks in the Kemum Block [81]. Instead, these have been interpreted to share similar zircon spectra age peaks to those from northern Queensland and the Queensland Plateau [71,80,83]. Comparisons of the biostratigraphy of wells from the Laura Basin, North Queensland (Marina-1), and the Lengguru Fold and Thrust Belt (Kamakawala-1X) are similarly interpreted to share biostratigraphic (palynological) events during the Early Cretaceous [80].

The interpreted middle Cretaceous location for the origin of the Papuan Peninsula is significant given the volcaniclastic provenance for the sedimentary material. It has previously been interpreted that erosion of the Australian continent and widespread Aptian–Cenomanian volcanism along its northern and eastern margins [3,24,84–86] led to the accumulation of a $\geq$10 km thick volcano–sedimentary sequence atop the rifted continental crust of the Australian Plate. This sequence included the protolith of the Owen Stanely Metamorphics of the Papuan Peninsula, and significantly, the Whitsunday Volcanic Province [87,88]. Early–middle Cretaceous (ca. 135–95 Ma) magmatic products along the eastern margin of Australia define the Whitsunday Volcanic Province, with a main period of igneous activity dated between 120 and 105 Ma [89]. Bryan et al. [89] outlines that the early phases of volcanism (ca. 130–115 Ma) were dominantly dacitic to rhyolitic magmas, with later stages (<115 Ma) being bimodal in composition and mafic magma compositions progressively less contaminated with time, with intrusion of primitive E-MORB gabbros occurring later in the igneous history. This compares well with the results of Osterle et al. [24], who found the Albian to Upper Cretaceous Goropu Metabasalt and Emo Metamorphics of the Papuan Peninsula fall within and above a geochemical MORB-OIB array, with an interpreted contamination by either continental crust [90] or supra subduction zone processes [20]. Based on the interpreted location, timing, and composition of Papuan Peninsula volcanism, we suggest that these could be considered part of the Central Queensland Whitsunday Volcanic Province prior to, and during, break-up and rifting of the eastern Australian margin.

A full tectonic reconstruction to account for the findings of this study is out of scope for the current work. However, Gold et al. [80] have attempted a first-pass interpretation for a tectonic reconstruction that could account for the findings presented here. In their model, the Papuan Peninsula rifts from the Australian margin at approximately 100 Ma, which constrains the timing for onset of rifting from northeastern Australia, is also the approximate depositional age for the protolith of the Owen Stanley Metamorphics [8,9].

7. Conclusions

In this study we report the results of an investigation into Miocene–Pliocene volcanic and volcaniclastic rocks of the Papuan Peninsula. Zircon U-Pb dating was conducted on samples derived from the Apinaipi Formation, Astrolabe Agglomerate, Mt Davidson Volcanics, Yaifa Formation, and the Kore Volcanics. The results of the U-Pb zircon geochronology are compiled from 1050 analyzed zircon grains that yielded 803 concordant ages. Results from the U–Pb zircon geochronology returned ages ranging from the middle Pliocene up to the Paleoarchean. Most samples yielded Miocene–Pliocene zircon grains, with the majority between middle Miocene and Pliocene in age. These results inform the recent geological history of the Papuan Peninsula with magmatism active during the late Miocene and early Pliocene, between approximately 9 Ma and 4.5 Ma.

The majority of zircon grains analyzed were inherited with 582 concordant zircon analyses dated as Cretaceous to Paleoarchean in age. Four of the five sampled Miocene–Pliocene volcanic and volcaniclastic formations selected for this study yielded sufficient Cretaceous zircon to derive protolith maximum depositional ages, between ca. 103 Ma and 100 Ma. This is interpreted as a maximum depositional age of the Owen Stanely Metamorphics, the basement of the Papuan Peninsula, and the most likely source of the inherited zircon grains. We compared the inherited zircon age spectra with the zircon age spectra and crustal history of possible source regions. The zircon U-Pb age spectra are most similar to a probable source region adjacent to the Shoalwater Formation of the Central Queensland margin and New Caledonia and are notably dissimilar to age spectra from North Queensland, Australia, inferred as the source of detritus by current plate tectonic models. We therefore interpret that the protolith to the basement of the Papuan Peninsula—the Owen Stanely Metamorphics—formed as a middle-Cretaceous volcaniclastic belt deposited to the east of present day Central Queensland, and formed part of the wider Whitsunday Igneous Event during break-up and rifting of the Tasman Sea and Coral Sea.

Supplementary Materials: The following supporting information can be downloaded at: https://www.mdpi.com/article/10.3390/geosciences13110324/s1, Figure S1: Zircon CL Images 1; Figure S2: Zircon CL Images 2; Figure S3: Zircon CL Images 3; Figure S4: Zircon CL Images 4; Figure S5: Zircon CL Images 5; Table S1: Zircon U-Pb Data.

Author Contributions: Conceptualization, R.J.H. and D.S.; Data curation, R.J.H.; Formal analysis, R.J.H. and K.H.; Funding acquisition, R.J.H.; Investigation, R.J.H.; Methodology, R.J.H., K.H. and D.S.; Project administration, R.J.H.; Resources, R.J.H. and G.M.; Validation, R.J.H. and K.H.; Visualization, R.J.H. and G.M.; Writing—original draft, R.J.H.; Writing—review and editing, R.J.H., K.H., D.S. and G.M. All authors have read and agreed to the published version of the manuscript.

Funding: This research was funded by the 34th IGC Travel Grant Scheme for Early-Career Australian and New Zealand Geoscientists from the Australian Geoscience Council and the Australian Academy of Science, and the James Cook University Early Career Researcher Rising Stars Leadership Program.

Data Availability Statement: Data generated as part of this study are included in the body of the article or available in the Supplementary Material.

Acknowledgments: The editor and reviewers are thanked for their comments and suggestions. Nathan Mosusu, and staff of the Mineral Resources Authority are thanked for their assistance with fieldwork and logistics. John Wardell is thanked for assisting with rock processing; Yi Hu and staff of the Advanced Analytical Centre, JCU are also acknowledged for support with analytical work. David Gold and Lloyd White are thanked for discussions on the study.

Conflicts of Interest: The authors declare no conflict of interest. The funders had no role in the design of the study; in the collection, analyses, or interpretation of data; in the writing of the manuscript; or in the decision to publish the results.

Appendix A

Figure A1. Photo of rock samples used in this study. Sample locations and descriptions are included in Table 1.

Appendix B

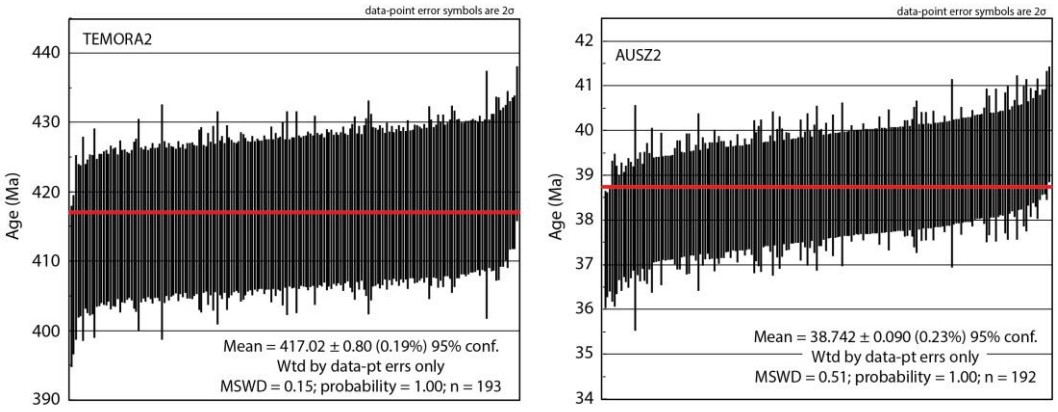

Figure A2. U-Pb dating secondary standard plots.

References

1. Honza, E.; Davies, H.L.; Keene, J.B.; Tiffin, D.L. Plate boundaries and evolution of the Solomon Sea region. *Geo-Mar. Lett.* **1987**, *7*, 161–168. [CrossRef]
2. Smith, R.I. Tertiary Plate Tectonic Setting and Evolution of Papua New Guinea. In *Petroleum Exploration in Papua New Guinea: Proceedings of the First PNG Petroleum Convention, Port Moresby, Papua New Guinea, 12–14 February 1990*; Carman, G.J., Carman, Z., Eds.; AAPG: Tulsa, OK, USA, 1990; pp. 229–244.
3. Hill, K.C.; Hall, R. Mesozoic-Cenozoic evolution of Australia's New Guinea margin in a west Pacific context. Geological Society of Australia Special Publication 22. *Geol. Soc. Am. Spec. Pap.* **2003**, *372*, 265–289.
4. Pigram, C.J.; Symonds, P.A. A review of the timing of the major tectonic events in the New Guinea Orogen. *J. Southeast Asian Earth Sci.* **1991**, *6*, 307–318. [CrossRef]
5. Davies, H.L. The geology of New Guinea—The cordilleran margin of the Australian continent. *Episodes* **2012**, *35*, 87–102. [CrossRef]
6. Holm, R.J.; Tapster, S.; Jelsma, H.A.; Rosenbaum, G.; Mark, D.F. Tectonic evolution and copper-gold metallogenesis of the Papua New Guinea and Solomon Islands region. *Ore Geol. Rev.* **2019**, *104*, 208–226. [CrossRef]
7. Van Wyck, N.; Williams, I.S. Age and provenance of basement metasediments from the Kubor and Bena Bena Blocks, central Highlands, Papua New Guinea: Constraints on the tectonic evolution of the northern Australian cratonic margin. *Aust. J. Earth Sci.* **2002**, *49*, 565–577. [CrossRef]
8. Kopi, G.; Williams, I.; Findlay, R.H. *New Detrital Zircon Data from the Wau-Bulolo Region, Morobe Province, Papua New Guinea*; Geological Survey Technical Note 16/2004; Papua New Guinea Department of Mining: Port Moresby, Papua New Guinea, 2004.
9. Holm, R.J.; Poke, B. Petrology and crustal inheritance of the Cloudy Bay Volcanics as derived from a fluvial conglomerate, Papuan Peninsula (Papua New Guinea): An example of geological inquiry in the absence of in situ outcrop. *Cogent Geosci.* **2018**, *4*, 1450198. [CrossRef]
10. Hall, R. Cenozoic geological and plate tectonic evolution of SE Asia and the SW Pacific: Computer-based reconstructions, model and animations. *J. Asian Earth Sci.* **2002**, *20*, 353–431. [CrossRef]
11. Seton, M.; Müller, R.D.; Zahirovic, S.; Gaina, C.; Torsvik, T.H.; Shephard, G.; Talsma, A.; Gurnis, M.; Turner, M.; Maus, S.; et al. Global continental and ocean basin reconstructions since 200 Ma. *Earth-Sci. Rev.* **2012**, *113*, 212–270. [CrossRef]
12. Zahirovic, S.; Matthews, K.J.; Flament, N.; Müller, R.D.; Hill, K.C.; Seton, M.; Gurnis, M. Tectonic evolution and deep mantle structure of the eastern Tethys since the latest Jurassic. *Earth-Sci. Rev.* **2016**, *162*, 293–337. [CrossRef]
13. Gaina, C.; Müller, D.R.; Royer, J.-Y.; Symonds, P. Evolution of the Louisiade triple junction. *J. Geophys. Res.* **1999**, *104*, 12927–12939. [CrossRef]
14. Schellart, W.P.; Lister, G.S.; Toy, V.G. A Late Cretaceous and Cenozoic reconstruction of the Southwest Pacific region: Tectonics controlled by subduction and slab rollback processes. *Earth-Sci. Rev.* **2006**, *76*, 191–233. [CrossRef]
15. Webb, L.E.; Baldwin, S.L.; Fitzgerald, P.G. The Early-Middle Miocene subduction complex of the Louisiade Archipelago, southern margin of the Woodlark Rift. *Geochem. Geophys. Geosyst.* **2014**, *15*, 4024–4046. [CrossRef]
16. Holm, R.J.; Spandler, C.; Richards, S.W. Continental collision, orogenesis and arc magmatism of the Miocene Maramuni arc, Papua New Guinea. *Gondwana Res.* **2015**, *28*, 1117–1136. [CrossRef]
17. Gehrels, G. Detrital Zircon U-Pb Geochronology Applied to Tectonics. *Annu. Rev. Earth Planet. Sci.* **2014**, *42*, 127–149. [CrossRef]
18. Pieters, P.E. *Port Moresby-Kalo-Aroa, Papua New Guinea—1:250,000 Geological Map Series*, BMR Australia Explanatory Notes; BMR Australia. 1978; 55p.
19. Worthing, M.A.; Crawford, A.J. The igneous geochemistry and tectonic setting of metabasites from the emo metamorphics, Papua New Guinea; A record of the evolution and destruction of a backarc basin. *Miner. Pet.* **1996**, *58*, 79–100. [CrossRef]

20. Smith, I.E.M. The chemical characterization and tectonic significance of ophiolite terrains in southeastern Papua New Guinea. *Tectonics* **2013**, *32*, 159–170. [CrossRef]
21. Kopi, G.; Findlay, R.H.; Williams, I. Age and provenance of the Owen Stanley Metamorphic Complex, East Papuan Composite Terrane, Papua New Guinea: Geological Survey of Papua New Guinea, Report. 2000; *unpublished*.
22. Dow, D.B.; Smit, J.A.J.; Page, R.W. Wau—1:250 2000,000 Geological Series. Explanatory notes to accompany Wau 1:250,000 geological map: Geological Survey of Papua New Guinea, Explanatory Notes SB/55-14. 1974.
23. Smith, I.E.M.; Davies, H.L. Geology of the southeast Papuan mainland. *BMR J. Aust. Geol. Geophys.* **1976**, *165*, 86.
24. Österle, J.; Little, T.; Seward, D.; Stockli, D.; Gamble, J. The petrology, geochronology and tectono-magmatic setting of igneous rocks in the Suckling-Dayman metamorphic core complex, Papua New Guinea. *Gondwana Res.* **2020**, *83*, 390–414. [CrossRef]
25. Baldwin, S.L.; Fitzgerald, P.G.; Webb, L.E. Tectonics of the New Guinea Region. *Annu. Rev. Earth Planet. Sci.* **2012**, *40*, 495–520. [CrossRef]
26. Davies, H.L.; Jaques, A.L. Emplacement of ophiolite in Papua New Guinea. *Geol. Soc. Lond. Spec. Publ.* **1984**, *13*, 341–349. [CrossRef]
27. Davies, H.L.; Smith, I.E. Geology of Eastern Papua. *Geol. Soc. Am. Bull.* **1971**, *82*, 3299–3312. [CrossRef]
28. Lus, W.Y.; McDougall, I.; Davies, H.L. Age of the metamorphic sole of the Papuan Ultramafic Belt ophiolite, Papua New Guinea. *Tectonophysics* **2004**, *394*, 85–101. [CrossRef]
29. Jakes, P.; Smith, I.E.M. High potassium calc–alkaline rocks from Cape Nelson, Eastern Papua. *Contrib. Mineral. Petrol.* **1970**, *28*, 259–271. [CrossRef]
30. Smith, I.E. High-potassium intrusive from southeast Papua. *Contrib. Mineral. Petrol.* **1972**, *34*, 167–176. [CrossRef]
31. Smith, I.E. Volcanic evolution of eastern Papua. *Tectonophysics* **1982**, *87*, 315–334. [CrossRef]
32. Smith, I.E.M. High-Magnesium Andesites: The Example of the Papuan Volcanic Arc. In *Orogenic Andesites and Crustal Growth*; Gómez-Tuena, A., Straub, S.M., Zellmer, G.F., Eds.; Geological Society; Special Publications: London, UK, 2013; p. 385.
33. Smith, I.E.; Milsom, J.S. Late Cenozoic volcanism and extension in Eastern Papua. *Geol. Soc. Lond. Spéc. Publ.* **1984**, *16*, 163–171. [CrossRef]
34. Luyendyk, B.P.; MacDonald, K.C.; Byran, W.B. Rifting history of the Woodlark Basin in the southwest Pacific. *Geol. Soc. Am. Bull.* **1973**, *84*, 1125–1134. [CrossRef]
35. Smith, I.E.M.; Chappell, B.W.; Ward, G.K.; Freeman, R.S. Peralkaline rhyolites associated with andesitic arcs of the southwest Pacific. *Earth Planet. Sci. Lett.* **1977**, *37*, 230–236. [CrossRef]
36. Ibañez-Mejia, M.; Pullen, A.; Pepper, M.; Urbani, F.; Ghoshal, G.; Ibañez-Mejia, J.C. Use and abuse of detrital zircon U-Pb geochronology—A case from the Rio Orinoco delta, eastern Venezuela. *Geology* **2018**, *46*, 1019–1022. [CrossRef]
37. Sircombe, K.N.; Bleeker, W.; Stern, R.A. Detrital zircon geochronology and grain-size analysis of a ~2800 Ma Mesoarchean protocratonic cover succession, Slave Province, Canada. *Earth Planet. Sci. Lett.* **2001**, *189*, 207–220. [CrossRef]
38. Garzanti, E.; Andò, S.; Vezzoli, G. Grainsize dependence of sediment composition and environmental bias in provenance studies. *Earth Planet. Sci. Lett.* **2009**, *277*, 422–432. [CrossRef]
39. Hajek, E.A.; Huzurbazar, S.V.; Mohrig, D.; Lynds, R.M.; Heller, P.L. Statistical characterization of grain-size distributions in sandy fluvial systems. *J. Sediment. Res.* **2010**, *80*, 184–192. [CrossRef]
40. Lawrence, R.L.; Cox, R.; Mapes, R.W.; Coleman, D.S. Hydrodynamic fractionation of zircon age populations. *Geol. Soc. Am. Bull.* **2011**, *123*, 295–305. [CrossRef]
41. Skwarko, S.K. Stratigraphic Tables, Papua New Guinea. Bureau of Mineral Resources 1978, Geology and Geophysics, Australia, Report 193, BMR Microfilm MF61.
42. Holm, R.J.; Spandler, C.; Richards, S.W. Melanesian arc far-field response to collision of the Ontong Java Plateau: Geochronology and pertrogenesis of the Simuku Igneous Complex, New Britain, Papua New Guinea. *Tectonophysics* **2013**, *603*, 189–212. [CrossRef]
43. Van Achterbergh, E.; Ryan, C.G.; Jackson, S.E.; Griffin, W.L. *Appendix, Laser Ablation-ICP-Mass Spectrometry in the Earth Sciences: Principle and Applications*; Short Course Series; Sylvester, P.J., Ed.; Mineralogical Association of Canada (MAC): Ottawa, ON, Canada, 2001; Volume 29, p. 239.
44. Jackson, S.E.; Pearson, N.J.; Griffin, W.L.; Belousova, E.E. The application of laser ablation-inductively coupled plasma-mass spectrometry to in situ U-Pb zircon geochronology. *Chem. Geol.* **2004**, *211*, 47–69. [CrossRef]
45. Black, L.P.; Kamo, S.L.; Allen, C.M.; Davis, D.W.; Aleinkoff, J.N.; Valley, J.W.; Mudil, R.; Campbell, I.H.; Korsch, R.J.; Williams, I.S.; et al. Improved 206Pb/238U microprobe geochronology by the monitoring of trace-element-related matrix effect; SHRIMP, ID-TIMS, ELA-ICP-MS and oxygen isotope documentation for a series of zircon standards. *Chem. Geol.* **2004**, *205*, 115–140. [CrossRef]
46. Kennedy, A.K.; Wotzlaw, J.-F.; Schaltegger, U.; Crowley, J.L.; Schmitz, M. Eocene zircon reference material for microanalysis of U-Th-Pb isotopes and trace elements. *Can. Mineral.* **2014**, *52*, 409–421. [CrossRef]
47. Ludwig, K.R. User's Manual for Isoplot 3.70: A Geochronological Toolkit for Microsoft Excel. In *Berkeley Geochronology Center Special Publication No. 4*; Berkeley Geochronology Center: Berkeley, CA, USA, 2009.
48. Schärer, U. The effect of initial 230Th disequilibrium on young U-Pb ages: The Makalu case, Himalaya. *Earth Planet. Sci. Lett.* **1984**, *67*, 191–204. [CrossRef]
49. Parrish, R.R. U-Pb dating of monazite and its application to geological problems. *Can. J. Earth Sci.* **1990**, *27*, 1431–1450. [CrossRef]

50. Crowley, J.L.; Schoene, B.; Bowring, S.A. U-Pb dating of zircon in the Bishop Tuff at the millennial scale. *Geology* **2007**, *35*, 1123–1126. [CrossRef]
51. Tera, F.; Wasserburg, G.J. U-Th-Pb systematics in three Apollo 14 basalts and the problem of initial Pb in lunar rocks. *Earth Planet. Sci. Lett.* **1972**, *14*, 281–304. [CrossRef]
52. Stacey, J.S.; Kramers, J.D. Approximation of terrestrial lead isotope evolution by a two-stage model. *Earth Planet. Sci. Lett.* **1975**, *26*, 207–221. [CrossRef]
53. Coutts, D.S.; Matthews, W.A.; Hubbard, M. Assessment of widely used methods to derive depositional ages from detrital zircon populations. *Geosci. Front.* **2019**, *10*, 1421–1435. [CrossRef]
54. Vermeesch, P. Maximum depositional age estimation revisited. *Geosci. Front.* **2021**, *12*, 843–850. [CrossRef]
55. Dickinson, W.R.; Gehrels, G.E. U-Pb ages of detrital zircons in Jurassic eolian and associated sandstones of the Colorado plateau: Evidence for transcontinental dispersal and intraregional recycling of sediment. *GSA Bull.* **2009**, *121*, 408–433. [CrossRef]
56. Ross, J.B.; Ludvigson, G.A.; Möller, A.; Gonzales, L.A.; Walker, J.D. Stable isotope paleohydrology and chemostratigraphy of the Albian Wayan Formation of the wedge-top depozone, North American western interior basin. *Sci. China Earth Sci.* **2017**, *60*, 44–57. [CrossRef]
57. Vermeesch, P. IsoplotR: A free and open toolbox for geochronology. *Geosci. Front.* **2018**, *9*, 1479–1493. [CrossRef]
58. Vermeesch, P. On the visualisation of detrital age distributions. *Chem. Geol.* **2012**, *312–313*, 190–194.
59. Ahrens, L.H.; Cherry, R.D.; Erlank, A.J. Observations on the Th-U relationship in zircons from granitic rocks and from kimberlites. *Geochem. Cosmochim. Acta* **1967**, *29*, 711–716. [CrossRef]
60. Corfu, F.; Hanchar, J.M.; Hoskin, P.W.O.; Kinny, P. Atlas of Zircon Textures. In *Reviews in Mineralogy & Geochemistry 53: Zircon*; Hanchar, J.M., Hoskin, P.W.O., Eds.; Mineralogical Society of America: Chantilly, VA, USA, 2003.
61. Heaman, L.M.; Bowins, R.; Crocket, J. The chemical composition of igneous zircon suites: Implications for geochemical tracer studies. *Geochim. Cosmochim. Acta* **1990**, *54*, 1597–1607. [CrossRef]
62. Hoskin, P.W.O.; Schaltegger, U. The Composition of Zircon and Igneous and Metamorphic Petrogenesis. In *Reviews in Mineralogy & Geochemistry 53: Zircon*; Hanchar, J.M., Hoskin, P.W.O., Eds.; Mineralogical Society of America: Chantilly, VA, USA, 2003.
63. Ashley, P.M.; Flood, R.H. Low-K tholeiites and high-K igneous rocks from Woodlark Island, Papua New Guinea. *J. Geol. Soc. Aust.* **1981**, *28*, 227–240. [CrossRef]
64. Bodorkos, S.; Sheppard, S.; Saroa, D.; Tsiperau, C.U.; Sircombe, K.N. *New SHRIMP U-Pb Zircon Ages from the Wau-BulolоRegion, Papua New Guinea*; Geoscience Australia Record 2013/25; Papua New Guinea Technical Note TN 2013/05; Mineral Resources Authority: Port Moresby, Papua New Guinea, 2013.
65. Blewett, R.S.; Black, L.P.; Sun, S.-S.; Knutson, J.; Hutton, L.J.; Bain, J.H.C. U-Pb zircon and Sm-Nd geochronology of the Mesoproterozoic of North Queensland: Implications for a Rodian connection with the Belt supergroup of North America. *Precambrian Res.* **1998**, *89*, 101–127. [CrossRef]
66. Murgulov, V.; Beyer, E.; Griffin, W.L.; O'Reilly, S.Y.; Walters, S.G.; Stephens, D. Crustal evolution in the Georgetown Inlier, North Queensland, Australia: A detrital zircon grain study. *Chem. Geol.* **2007**, *245*, 198–218. [CrossRef]
67. Shaanan, U.; Rosenbaum, G.; Sihombing, F.M.H. Continuation of the Ross-Delamerian Orogen: Insights from eastern Australian detrital-zircon data. *Aust. J. Earth Sci.* **2017**, *65*, 1123–1131. [CrossRef]
68. Cheng, Y.; Todd, C.N.; Henderson, R.A.; Danišík, M.; Sahlström, F.; Chang, Z.; Corral, I. Jurassic uplift and erosion of the northeast Queensland continental margin: Evidence from (U–Th)/He thermochronology combined with U–Pb detrital zircon age spectra. *Aust. J. Earth Sci.* **2020**, *67*, 591–604. [CrossRef]
69. Tucker, R.T.; Roberts, E.M.; Henderson, R.A.; Kemp, A.I. Large igneous province or long-lived magmatic arc along the eastern margin of Australia during the Cretaceous? Insights from the sedimentary record. *GSA Bull.* **2016**, *128*, 1461–1480. [CrossRef]
70. Korsch, R.J.; Adams, C.J.; Black, L.P.; Foster, D.A.; Fraser, G.L.; Murray, C.G.; Foudoulis, C.; Griffin, W.L. Geochronology and provenance of the Late Paleozoic accretionary wedge and Gympie Terrane, New England Orogen, eastern Australia. *Aust. J. Earth Sci.* **2009**, *56*, 655–685. [CrossRef]
71. Shaanan, U.; Rosenbaum, G.; Hoy, D.; Mortimer, N. Late Paleozoic geology of the Queensland Plateau (offshore northeastern Australia). *Aust. J. Earth Sci.* **2018**, *65*, 357–366. [CrossRef]
72. Campbell, M.J.; Shaanan, U.; Rosenbaum, G.; Allen, C.M.; Cluzel, D.; Maurizot, P. Permian rifting and isolation of New Caledonia: Evidence from detrital zircon geochronology. *Gondwana Res.* **2018**, *60*, 54–68. [CrossRef]
73. Pirard, C.; Spandler, C. The zircon record of high-pressure metasedimentary rocks of New Caledonia: Implications for regional tectonics of the south-west Pacific. *Gondwana Res.* **2017**, *46*, 79–94. [CrossRef]
74. Rosenbaum, G. The Tasmanides: Phanerozoic tectonic evolution of eastern Australia. *Annu. Rev. Earth Planet. Sci.* **2018**, *46*, 291–325. [CrossRef]
75. Champion, D.C.; Bultitude, R.J. Kennedy Igneous Association. In *Geology of Queensland*; Jell, P.A., Ed.; Geological Survey of Queensland: Brisbane, QLD, Austrilia, 2013; pp. 473–514.
76. Matthews, K.J.; Maloney, K.T.; Zahirovic, S.; Williams, S.E.; Seton, M.; Muller, R.D. Global plate boundary evolution and kinematics since the late Paleozoic. *Glob. Planet. Change* **2016**, *146*, 226–250. [CrossRef]
77. Boyden, J.A.; Müller, R.D.; Gurnis, M.; Torsvik, T.H.; Clark, J.A.; Turner, M.; Ivey-Law, H.; Watson, R.J.; Cannon, J.S. Next-Generation Plate-Tectonic Reconstructions using GPlates. In *Geoinformatics: Cyberinfrastructure for the Solid Earth Sciences*; Keller, G.R., Baru, C., Eds.; Cambridge University Press: Cambridge, UK, 2011; pp. 95–114.

78. Little, T.A.; Webber, S.; Mizera, M.; Boulton, C.; Oesterle, J.; Ellis, S.; Boles, A.; Van der Pluijm, B.; Norton, K.; Seward, D.; et al. Evolution of a rapidly slipping, active low-angle normal fault, Suckling-Dayman metamorphic core complex, SE Papua New Guinea. *GSA Bull.* **2019**, *131*, 1333–1363. [CrossRef]
79. Klootwijk, C.; Giddings, J.; Pigram, C.; Loxton, C.; Davies, H.; Rogerson, R.; Falvey, D. Papua New Guinea Highlands: Palaeomagnetic constraints on terrane tectonics. *Tectonophysics* **2003**, *362*, 239–272. [CrossRef]
80. Gold, D.P.; Casas-Gallego, M.; Holm, R.; Webb, M.; White, L.T. New Tectonic Reconstructions of New Guinea Derived from Biostratigraphy and Geochronology. In Proceedings of the Indonesian Petroleum Association, Digital Technology Conference, Jakarta, Indonesia, 14–17 September 2020. 26p.
81. Decker, J.; Ferdian, F.; Morton, A.; Fanning, M.; White, L.T. New Geochronology Data from Eastern Indonesia—An Aid to Understanding Sedimentary Provenance in a Frontier Region. In Proceedings of the Indonesian Petroleum Association 41st Annual Convention & Exhibition 2017, IPA17-551-G, Jakarta, Indonesia, 17–19 May 2017. 18p.
82. Webb, M.; White, L.T.; Jost, B.M.; Tiranda, H. The Tamrau Block of NW New Guinea records late Miocene-Pliocene collision at the northern tip of the Australian Plate. *J. Asian Earth Sci.* **2019**, *179*, 238–260. [CrossRef]
83. Holm, R.; Gold, D.; White, L.; Webb, M.; Mahoney, L.; McLaren, S.; Heilbronn, K.; Oesterle, J.; Mizera, M.; Saroa, D.; et al. Provenance and Tectonics of the Allochthonous New Guinea Terranes: Implications for the Formation and Evolution of Regional Basins. In Proceedings of the 1st AAPG/EAGE PNG Geoscience Conference & Exhibition, Port Moresby, Papua New Guinea, 25–27 February 2020.
84. Dow, D.B. *A Geological Synthesis of Papua New Guinea*; Geology and Geophysics, Bulletin 201; Bureau of Mineral Resources: Canberra, ACT, Australia, 1977; 58p.
85. Dow, D.B.; Smit, J.A.J.; Bain, J.H.C.; Ryburn, R.J. Geology of the South Sepik Region, New Guinea. Geology and Geophysics, Bulletin 133, Bulletin PNG 4; Department of National Development, Bureau of Mineral Resources: Osborne Park, WA, Australia, 1972; 109p.
86. Hill, K.C.; Gleadow, A.J.W. Apatite Fission Track Analysis of the Papuan Basin. In *Petroleum Exploration and Development in Papua New Guinea: Proceedings of the First PNG Petroleum Convention*; Carman, G.J., Carman, Z., Eds.; PNG Chamber of Mines and Petroleum: Port Moresby, Papua New Guinea, 1990; pp. 119–136.
87. Bryan, S.E.; Constantine, A.E.; Stephens, C.J.; Ewart, A.; Schön, R.W.; Parianos, J. Early Cretaceous volcano-sedimentary successions along the eastern Australian continental margin: Implications for the break-up of eastern Gondwana. *Earth Planet. Sci. Lett.* **1997**, *153*, 85–102. [CrossRef]
88. Ewart, A.; Schon, R.W.; Chappell, B.W. The Cretaceous volcanic-plutonic province of the central Queensland (Australia) coast—A rift related 'calc-alkaline' province. *Earth Environ. Sci. Trans. R. Soc. Edinb.* **1992**, *83*, 327–345.
89. Bryan, S.E.; Cook, A.G.; Allen, C.M.; Siegel, C.; Purdy, D.J.; Greentree, J.S.; Uysal, I.T. Early-mid Cretaceous tectonic evolution of eastern Gondwana: From silicic LIP magmatism to continental rupture. *Episodes* **2012**, *35*, 142–152. [CrossRef]
90. Whattam, S.A. Arc-continent collisional orogenesis in the SW Pacific and the nature, source and correlation of emplaced ophiolitic nappe components. *Lithos* **2009**, *113*, 88–114. [CrossRef]

Disclaimer/Publisher's Note: The statements, opinions and data contained in all publications are solely those of the individual author(s) and contributor(s) and not of MDPI and/or the editor(s). MDPI and/or the editor(s) disclaim responsibility for any injury to people or property resulting from any ideas, methods, instructions or products referred to in the content.